JOURNAL OF SCIENCE

PART A: ENGINEERING AND INNOVATION

GAZİ UNIVERSITY

1926

Year | Yıl: **2022** **Volume** | Cilt: **9** **Issue** | Sayı: **1**

e-ISSN 2147-9542

Gazi University
Journal of Science
PART A: ENGINEERING AND INNOVATION
e-ISSN 2147-9542
YEAR YIL 2022 VOLUME CİLT 9 ISSUE SAYI 1

Gazi University
Journal of Science
PART A: ENGINEERING AND INNOVATION

e-ISSN 2147-9542 | YEAR YIL 2022 | VOLUME CİLT 9 | ISSUE SAYI 1

Associate Editors | Alan Editörleri

Gazi University
Journal of Science
PART A: ENGINEERING AND INNOVATION

e-ISSN 2147-9542 | YEAR YIL 2022 | VOLUME CİLT 9 | ISSUE SAYI 1

Associate Editors | Alan Editörleri

Gazi University
Journal of Science
PART A: ENGINEERING AND INNOVATION
e-ISSN 2147-9542
YEAR YIL 2022 VOLUME CİLT 9 ISSUE SAYI 1

Gazi University
Journal of Science
PART A: ENGINEERING AND INNOVATION

e-ISSN 2147-9542 | YEAR YIL 2022 | VOLUME CİLT 9 | ISSUE SAYI 1

Correspondence Address

Gazi University Graduate School of Natural and Applied Sciences
Emniyet Neighborhood, Bandırma Avenue, No:6/20B, 06560, Yenimahalle - ANKARA
B Block, Auxiliary Building

Yazışma Adresi

Gazi Üniversitesi Fen Bilimleri Enstitüsü
Emniyet Mahallesi, Bandırma Caddesi, No:6/20B, 06560, Yenimahalle - ANKARA
B Blok, Ek Bina

e-mail | e-posta

gujsa06@gmail.com

web page | web sayfası

https://dergipark.org.tr/tr/pub/gujsa

Gazi University Journal of Science Part A: Engineering and Innovation is a peer-reviewed journal.

Gazi Üniversitesi Fen Bilimleri Dergisi Bölüm A: Mühendislik ve İnovasyon hakemli bir dergidir.

Gazi University
Journal of Science
PART A: ENGINEERING AND INNOVATION
e-ISSN 2147-9542
YEAR YIL 2022 VOLUME CİLT 9 ISSUE SAYI 1

INDEXING | DİZİNLENME

ACCESSIBILITY | ERİŞİLEBİLİRLİK

Gazi University
Journal of Science
PART A: ENGINEERING AND INNOVATION

e-ISSN 2147-9542

YEAR YIL 2022 VOLUME CİLT 9 ISSUE SAYI 1

CONTENTS | İÇİNDEKİLER

Research Article / Araştırma Makalesi GU J Sci, Part A, 9(1): 1-11 (2022) https://doi.org/10.54287/gujsa.1029633

Gazi University
Journal of Science
PART A: ENGINEERING AND INNOVATION
http://dergipark.org.tr/gujsa

Investigating (p,q)-hybrid Durrmeyer-type Operators in terms of Their Approximation Properties

Ülkü DİNLEMEZ KANTAR[1*], İsmet YÜKSEL[1]

[1]*Gazi University, Faculty of Science, Department of Mathematics, Ankara, Turkey*

Keywords
(p,q)-hybrid operators
(p,q)-calculus
rates of approximation
q-Stancu type operators
weighted approximation

Abstract
This study introduces (p,q)-hybrid Durrmeyer-Stancu type linear positive operators, which are generalized forms of q-hybrid Durrmeyer-Stancu-type linear positive operators and examines their approximation properties. The first modulus of continuity on a finite interval is introduced using Peetre's K-functional. Then, the weighted approximation theorem in a weighted space is provided using Gadzhiev's weighted Korovkin-type theorem. Finally, these operators' rates of convergence are obtained for the continuous functions.

Cite
Dinlemez Kantar, U., & Yuksel, I. (2022). Investigating (p,q)-hybrid Durrmeyer-type operators in terms of their approximation properties. *GU J Sci, Part A, 9*(1), 1-11.

Author ID (ORCID Number)
Ü. Dinlemez Kantar, 0000-0002-5656-3924
İ. Yüksel, 0000-0002-2631-2382

Article Process
Submission Date 28.11.2021
Revision Date 04.01.2022
Accepted Date 19.01.2022
Published Date 25.01.2022

1. INTRODUCTION

In Dinlemez et al. (2014), they introduced q −hybrid Durrmeyer-Stancu type linear positive operators for $0 < q \leq 1$ as

$$H_{m,q}^{\alpha,\beta}(g,x) = \sum_{k=1}^{\infty} s_{m,k,q}(x) \int_0^{\infty/A} b_{m,k-1,q}(t) g\left(\frac{[m]_q t + \alpha}{[m]_q + \beta}\right) d_q t + e^{-[m]_q x} g\left(\frac{\alpha}{[m]_q + \beta}\right), \tag{1}$$

where

$$s_{m,k,q}(x) = \frac{e^{-[m]_q x}[m-1]_q}{[k]_q!}\left([m]_q x\right)^k,$$

and

$$b_{m,k,q}(x) = \begin{bmatrix} m+k-1 \\ k \end{bmatrix}_q q^{k(k-1)} \frac{x^k}{(1+x)_q^{m+k}}.$$

are q-Szász and q-Baskakov basis functions, respectively. A q −analogue of the Bernstein operators was introduced by Lupaş (1987). These operators were based on q-integer and q-binomial coefficients for the first time. Then, a number of interesting generalizations about q-calculus were studied by Jackson (1910), Koelink & Koornwinder (1990), Phillips (1997), Kac & Cheung (2002), De Sole & Kac (2005), Doğru & Gupta (2005, 2006), Gupta & Heping (2008), Gupta & Aral (2010), Gupta & Karsli (2012), Aral et al. (2013), Yüksel (2013).

*Corresponding Author, e-mail: ulku@gazi.edu.tr

Sahai & Yadav (2007), Kanat & Sofyalıoğlu (2018), Sofyalıoğlu et al. (2021) introduced the generalization of (p,q) −calculus. Recently, the series of studies on (p,q)-generalizations with a sequence of linear positive operators have been made by Mursaleen et al. (2015 a,b,c), Acar et al. (2016, 2018), Gupta (2018), Cai et al. (2021), Kanat & Sofyalıoğlu (2021). Our objective is going to obtain the generalization of (p,q) −calculus of hybrid Durrmeyer-Stancu type operators in Dinlemez et al. (2014).

2. PRELIMINARIES AND NOTATIONS

Some basic formulas in (p,q) −calculus in the literature can be obtained using basic q −calculus as follows

$$[m]_{p,q} = \frac{p^m - q^m}{p-q}, \qquad [m]_{p,q}! = [1]_{p,q}[2]_{p,q} \ldots . [m]_{p,q},$$

$$(a \oplus b)^{\,m}_{p,q} = (a+b)(ap+bq)(ap^2-bq^2)\ldots(ap^{m-1}-bq^{m-1}),$$

$$d_{p,q}f(x) = f(px) - f(qx), \qquad [m]_{p,q} = p^{m-1}[m]_{q/p},$$

$$[m]_{p,q}! = p^{\frac{m(m-1)}{2}}[m]_{q/p}!, \qquad (a \oplus b)^{\,m}_{p,q} = p^{\frac{m(m-1)}{2}}(a+b)^{\,m}_{q/p}.$$

We define the (p,q) −beta functions $B_{p,q}(k,m)$ as follows

$$B_{p,q}(k,m) = p^{\binom{m}{2}}q^{\binom{k}{2}}\int_0^{\infty/A}\frac{t^{k-1}}{(1+t)^{m+k}_{p,q}}d_{p,q}t, A>0 \text{ and } m,k \in \mathbb{N}. \tag{2}$$

3. (p,q) −HYBRID OPERATORS

Let $A > 0$, $k \in \mathbb{N}$, $m \in \mathbb{N} \setminus \{0\}$, and f is a continuous function with real-value in the interval $[0,\infty)$. Then, (p,q) − hybrid Durrmeyer-Stancu type linear positive operators are written for $0 < q < p \leq 1$ as follows

$$H^{\alpha,\beta}_{m,p,q}(g,x) = \sum_{k=1}^{\infty} s_{m,k,p,q}(x)\gamma_{m,k}(p,q)\int_0^{\infty/A} b_{m,k-1,p,q}(t)g\left(\frac{p^{-m}[m]_{p,q}t+\alpha}{[m]_{p,q}+\beta}\right)d_{p,q}t + e^{-[m]_{p,q}x}g\left(\frac{\alpha}{[m]_{p,q}+\beta}\right), \tag{3}$$

where

$$s_{m,k,p,q}(x) = \frac{e^{-[m]_{p,q}x}[m-1]_{p,q}}{[k]_{p,q}!}\left([m]_{p,q}x\right)^k,$$

$$b_{m,k,p,q}(x) = \begin{bmatrix} m+k-1 \\ k \end{bmatrix}_{p,q}\frac{x^k}{(1+x)^{m+k}_{p,q}},$$

and

$$\gamma_{m,k}(p,q) = q^{k(k-1)}p^{\binom{m-1}{2}}.$$

When we set $p = 1$ in (3), the operators $H^{\alpha,\beta}_{m,p,q}$ are reduced to q −hybrid Durrmeyer- Stancu type operators given in (1). Along with the manuscripts, the following notations will be used

$$R_{p,q}(m,\beta) = \left([m]_{p,q}+\beta\right), \qquad T_{p,q}(m,s) = \prod_{i=2}^{s}[m-i]_{p,q}.$$

And now the lemma for the Korovkin test functions can be given as follows:

Lemma1 When $e_r(t) = t^r,\ r = 0,1,2$, we get

(i) $H_{m,p,q}^{\alpha,\beta}(e_0, x) = 1$,

(ii) $H_{m,p,q}^{\alpha,\beta}(e_1, x) = \frac{p^{-2}[m]_{p,q}^2}{qR_{p,q}(m,\beta)T_{p,q}(m,2)}x + \frac{\alpha}{R_{p,q}(m,\beta)}$,

(iii) $H_{m,p,q}^{\alpha,\beta}(e_2, x) = \frac{p^{-3}[m]_{p,q}^4}{q^4\left(R_{p,q}(m,\beta)\right)^2 T_{p,q}(m,3)}x^2 + \left\{\frac{p^{-5}[2]_{p,q}[m]_{p,q}^3}{q^3\left(R_{p,q}(m,\beta)\right)^2 T_{p,q}(m,3)} + \frac{2\alpha p^{-3}[m]_{p,q}^2}{q\left(R_{p,q}(m,\beta)\right)^2 T_{p,q}(m,2)}\right\}x + \frac{\alpha^2}{\left(R_{p,q}(m,\beta)\right)^2}$

Proof After $(p, q) -$ beta functions in (2) are used, it is obtained as follows

$$\int_0^{\infty/A} b_{m,k-1,p,q}(t)t^r\, d_{p,q}t = \begin{bmatrix} m+k-2 \\ k-1 \end{bmatrix}_{p,q} \int_0^{\infty/A} \frac{t^{k+r-1}}{(1+t)_{p,q}^{m+k-1}} d_{p,q}t$$

$$= \frac{[k+r-1]_{p,q}!\,[m-r-2]_{p,q}!\, q^{-\binom{k+r}{2}}}{[m-1]_{p,q}!\,[k-1]_{p,q}!\, p^{\binom{m-r-1}{2}}}. \tag{4}$$

Then, by using (4) for $r = 0$, we obtain

$$H_{m,p,q}^{\alpha,\beta}(e_0, x) = \sum_{k=1}^{\infty} s_{m,k,p,q}(x)\gamma_{m,k}(p,q) \int_0^{\infty/A} b_{m,k-1,p,q}(t) d_{p,q}t + e^{-[m]_{p,q}x}$$

$$= e^{-[m]_{p,q}x} \sum_{k=0}^{\infty} \frac{\left([m]_{p,q}x\right)^k}{[k]_{p,q}!} q^{-k(k-1)/2}$$

$$= e^{-[m]_{p,q}x} E_{p,q}^{[m]_{p,q}x} = 1,$$

and the proof of (i) is completed. The following (ii) is obtained by a direct computation

$$H_{m,p,q}^{\alpha,\beta}(e_1, x) = \sum_{k=1}^{\infty} s_{m,k,p,q}(x)\gamma_{m,k}(p,q) \int_0^{\infty/A} b_{m,k-1,p,q}(t) \frac{p^{-m}[m]_{p,q}t + \alpha}{R_{p,q}(m,\beta)} d_{p,q}t + \frac{\alpha e^{-[m]_{p,q}x}}{R_{p,q}(m,\beta)}$$

$$= \frac{p^{-m}[m]_{p,q}}{R_{p,q}(m,\beta)T_{p,q}(m,2)} \sum_{k=1}^{\infty} \frac{\left([m]_{p,q}x\right)^k}{[k-1]_{p,q}!} q^{k(k-3)/2} p^{m-3} e^{-[m]_{p,q}x}$$

$$+ \frac{\alpha}{R_{p,q}(m,\beta)} \sum_{k=1}^{\infty} \frac{\left([m]_{p,q}x\right)^k}{[k]_{p,q}!} q^{k(k-1)/2} e^{-[m]_{p,q}x} + \frac{\alpha e^{-[m]_{p,q}x}}{R_{p,q}(m,\beta)}$$

$$= \frac{p^{-2}[m]_{p,q}^2}{qR_{p,q}(m,\beta)T_{p,q}(m,2)} x + \frac{\alpha}{R_{p,q}(m,\beta)}$$

Using the following equality

$$[s]_{p,q} = q^{s-r}[r]_{p,q} + p^r[s-r]_{p,q}, \qquad 0 \le r \le s, \tag{5}$$

we get

$$
\begin{aligned}
H^{\alpha,\beta}_{m,p,q}(e_2,x) &= \sum_{k=1}^{\infty} s_{m,k,p,q}(x)\gamma_{m,k}(p,q)\int_0^{\infty/A} b_{m,k-1,p,q}(t)\left(\frac{p^{-m}[m]_{p,q}t+\alpha}{R_{p,q}(m,\beta)}\right)^2 d_{p,q}t+\frac{\alpha^2 e^{-[m]_{p,q}x}}{\left(R_{p,q}(m,\beta)\right)^2} \\
&= \frac{p^{-2m}\left([m]_{p,q}\right)^2}{\left(R_{p,q}(m,\beta)\right)^2}\sum_{k=1}^{\infty} s_{m,k,p,q}(x)\gamma_{m,k}(p,q)\int_0^{\infty/A} b_{m,k-1,p,q}(t)t^2 d_{p,q}t \\
&+\frac{2\alpha p^{-m}[m]_{p,q}}{\left(R_{p,q}(m,\beta)\right)^2}\sum_{k=1}^{\infty} s_{m,k,p,q}(x)\gamma_{m,k}(p,q)\int_0^{\infty/A} b_{m,k-1,p,q}(t)t d_{p,q}t \\
&+\frac{\alpha^2}{\left(R_{p,q}(m,\beta)\right)^2}\sum_{k=1}^{\infty} s_{m,k,p,q}(x)\gamma_{m,k}(p,q)\int_0^{\infty/A} b_{m,k-1,p,q}(t)d_{p,q}t \\
&+\frac{\alpha^2 e^{-[m]_{p,q}x}}{\left(R_{p,q}(m,\beta)\right)^2} \\
&= \frac{p^{-3}[m]_{p,q}^4}{q^4\left(R_{p,q}(m,\beta)\right)^2 T_{p,q}(m,3)}x^2 \\
&+\left\{\frac{p^{-5}[2]_{p,q}[m]_{p,q}^3}{q^3\left(R_{p,q}(m,\beta)\right)^2 T_{p,q}(m,3)}+\frac{2\alpha p^{-3}[m]_{p,q}^2}{q\left(R_{p,q}(m,\beta)\right)^2 T_{p,q}(m,2)}\right\}x+\frac{\alpha^2}{\left(R_{p,q}(m,\beta)\right)^2}.
\end{aligned}
$$

Thus the proof of (iii) is completed.

For the main results of the study, we need to compute the second moment.

Lemma 2 Assuming that $0 < q < p \leq 1$ and $m > 3$, we obtain the following inequality

$$
H^{\alpha,\beta}_{m,p,q}((t-x)^2,x) \leq \left(\frac{2(1-p^{-2}q^3)}{q^4}+\frac{288(\alpha+\beta+1)^2[m]_{p,q}}{q^4 T_{p,q}(m,3)}\right)(x^2+x)+\frac{\alpha^2}{\left(R_{p,q}(m,\beta)\right)^2}.
$$

Proof To write the second moment, we use the result of Lemma 1 and the linearity of $H^{\alpha,\beta}_{m,p,q}$ operators;

$$
\begin{aligned}
H^{\alpha,\beta}_{m,p,q}((t-x)^2,x) &= \left\{\frac{p^{-3}[m]_{p,q}^4}{q^4\left(R_{p,q}(m,\beta)\right)^2 T_{p,q}(m,3)}-\frac{2p^{-2}[m]_{p,q}^2}{qR_{p,q}(m,\beta)T_{p,q}(m,2)}+1\right\}x^2 \\
&+\left\{\frac{p^{-5}[2]_{p,q}[m]_{p,q}^3+2\alpha q^2 p^{-3}[m-3]_{p,q}[m]_{p,q}^2}{q^3\left(R_{p,q}(m,\beta)\right)^2 T_{p,q}(m,3)}-\frac{2\alpha}{R_{p,q}(m,\beta)}\right\}x \\
&+\frac{\alpha^2}{\left(R_{p,q}(m,\beta)\right)^2} \\
&\leq \left\{\frac{[m]_{p,q}^4(p^{-3}+q^4)-2q^3p^{-2}[m-3]_{p,q}^4}{q^4\left(R_{p,q}(m,\beta)\right)^2 T_{p,q}(m,3)}\right. \\
&+\frac{q^4\left(q^{m-3}[3]_{p,q}+p^3[m-3]_{p,q}+\beta\right)^2\left(q^{m-3}+p[m-3]_{p,q}\right)[m-3]_{p,q}}{q^4\left(R_{p,q}(m,\beta)\right)^2 T_{p,q}(m,3)}
\end{aligned}
$$

$$+\frac{p^{-5}[2]_{p,q}[m]_{p,q}^3+2\alpha q^2p^{-3}[m-3]_{p,q}[m]_{p,q}^2}{q^3\left(R_{p,q}(m,\beta)\right)^2T_{p,q}(m,3)}\Bigg\}(x^2+x)$$
$$+\frac{\alpha^2}{\left(R_{p,q}(m,\beta)\right)^2}.$$

From (4), we have

$$\begin{aligned}H_{m,p,q}^{\alpha,\beta}((t-x)^2,x) &\le \Bigg\{\frac{2(1+p^{-2}q^3)[m-3]_{p,q}^4-2q^3p^{-2}[m-3]_{p,q}^4}{q^4\left(R_{p,q}(m,\beta)\right)^2T_{p,q}(m,3)}\\
&+\frac{\left(q^{m+1}p^6+2[3]_{p,q}p^4q^{m+1}+2p^4q^4\beta+4[3]_{p,q}p^6q^{m-3}\right)[m-3]_{p,q}^3}{q^4\left(R_{p,q}(m,\beta)\right)^2T_{p,q}(m,3)}\\
&+\frac{\left(pq^4\beta^2+2\beta pq^{m+1}\left(p^2+[3]_{p,q}\right)+2[3]_{p,q}p^3q^{2m-2}\right.}{q^4\left(R_{p,q}(m,\beta)\right)^2T_{p,q}(m,3)}\\
&+\frac{\left.[3]_{p,q}^2pq^{2m-2}(1+6p^3q^{-4})\right)[m-3]_{p,q}^2}{q^4\left(R_{p,q}(m,\beta)\right)^2T_{p,q}(m,3)}\\
&+\frac{\left(4[3]_{p,q}^3q^{3m-9}+[3]_{p,q}^2q^{3m-5}+\beta^2q^{m+1}+2\beta q^{2m-2}[3]_{p,q}\right)[m-3]_{p,q}}{q^4\left(R_{p,q}(m,\beta)\right)^2T_{p,q}(m,3)}\\
&+\frac{[3]_{p,q}^4p^{-3}q^{4m-12}+[m]_{p,q}^3[2]_{p,q}qp^{-5}+2\alpha p^{-3}q^3[m]_{p,q}^2[m-3]_{p,q}}{q^4\left(R_{p,q}(m,\beta)\right)^2T_{p,q}(m,3)}\Bigg\}(x^2+x)\\
&+\frac{\alpha^2}{\left(R_{p,q}(m,\beta)\right)^2}\\
&\le\left(\frac{2(1-p^{-2}q^3)}{q^4}+\frac{288(\alpha+\beta+1)^2[m]_{p,q}}{q^4T_{p,q}(m,3)}\right)(x^2+x)+\frac{\alpha^2}{\left(R_{p,q}(m,\beta)\right)^2}\end{aligned}$$

And the proof of the Lemma 2 is now completed.

Assume that, $B[0,\infty)$ denotes the set of all bounded functions from $[0,\infty)$ to $\mathbb{R}$. Having the norm $\|g\|_B=\sup\{|g(x)|: x\in[0,\infty)\}, B[0,\infty)$ is a normed space. For all continuous functions in $B[0,\infty)$, the subspace is denoted by $C_B[0,\infty)$. The first modulus of continuity on finite interval $[0,b]$, $b>0$ is denoted as follows;

$$w_{[0,b]}(g,\delta)=\sup_{0<h\le\delta,x\in[0,b]}|g(x+h)-g(x)|. \tag{6}$$

The Peetre's K-functional is defined with the help of the following representation

$$K_2(g,\delta)=\inf\{\|g-f\|_B+\delta\|f''\|_B: f\in W_\infty^2\},\qquad \delta>0 \tag{7}$$

where $W_\infty^2=\{f\in C_B[0,\infty): f',\ f''\in C_B[0,\infty)\}$. There is a positive constant C at Theorem 2.4 on p.177 in Gadzhiev (1976), such that

$$K_2(g,\delta) \leq C w_2(g,\sqrt{\delta}) \tag{8}$$

where

$$w_2(g,\sqrt{\delta}) = \sup_{0<h\leq\sqrt{\delta}} \sup_{x\in[0,b]} |g(x+2h) - g(x+h) - g(x)|. \tag{9}$$

In Gadzhiev (1976), Gadzhiev proved the weighted Korovkin-type theorems. Let $\sigma(x) = 1 + x^2$.

$B_\sigma[0,\infty)$ denotes the set of all functions g, from $[0,\infty)$ to $\mathbb{R}$ that meets the growth condition $|g(x)| \leq M_g \sigma(x)$.

In this inequality, M_g is a constant depending only on g. $B_\sigma[0,\infty)$ is a normed space with the norm

$\|g\|_\sigma = \sup\left\{\frac{|g(x)|}{\sigma(x)} : x \in [0,\infty)\right\}$. $C_\sigma[0,\infty)$ denotes the subspace of all continuous functions in $B_\sigma[0,\infty)$ and $C_\sigma^*[0,\infty)$ denotes the subspace of all functions $g \in C_\sigma[0,\infty)$ whose following limit exists finitely

$$\lim_{|x|\to\infty} \frac{|g(x)|}{\sigma(x)}.$$

Now, the direct results can be given. Because the following lemma is a routine, its proof is omitted.

Lemma 3 Let

$$\overline{H}_{m,p,q}^{\alpha,\beta}(g,x) = H_{m,p,q}^{\alpha,\beta}(g,x) - g\left(\frac{p^{-2}[m]_{p,q}^2}{qR_{p,q}(m,\beta)T_{p,q}(m,2)}x + \frac{\alpha}{R_{p,q}(m,\beta)}\right) + g(x). \tag{10}$$

For the operators (10), the following equalities are asserted:

(i) $\overline{H}_{m,p,q}^{\alpha,\beta}(1,x) = 1,$

(ii) $\overline{H}_{m,p,q}^{\alpha,\beta}(t,x) = x,$

(iii) $\overline{H}_{m,p,q}^{\alpha,\beta}(t-x,x) = 0.$

Lemma 4 Let $0 < q < p \leq 1$ and $m > 3$. Then $g'' \in C_B[0,\infty)$, we have the following inequality

$$\left|\overline{H}_{m,p,q}^{\alpha,\beta}(g,x) - g(x)\right| \leq \zeta_{m,p,q}^{\alpha,\beta}(x)\|g''\|_B$$

where $\zeta_{m,p,q}^{\alpha,\beta}(x) = \left(\frac{2(1-p^{-2}q^3)}{q^4} + \frac{332(\alpha+\beta+1)^2}{q^4 T_{p,q}(m,2)}\right)(x^2+x) + \frac{\alpha^2}{\left(R_{p,q}(m,\beta)\right)^2}.$

Proof Using Taylor's expansion

$$g(t) = g(x) + (t-x)g'(x) + \int_x^t (t-u)g''(u)du$$

and Lemma 3, we obtain

$$\overline{H}_{m,p,q}^{\alpha,\beta}(g,x) - g(x) = \overline{H}_{m,p,q}^{\alpha,\beta}\left(\int_x^t (t-u)g''(u)du, x\right).$$

Then, using Lemma1 and the following inequality

$$\left|\int_x^t (t-u)g''(u)du\right| \le \|g''\|_B \frac{(t-x)^2}{2},$$

we get

$$\begin{aligned}
\left|\overline{H}^{\alpha,\beta}_{m,p,q}(g,x)-g(x)\right| &\le \left|H^{\alpha,\beta}_{m,p,q}\left(\int_x^t (t-u)g''(u)du\,,x\right)\right. \\
&\left. - \int_x^{\frac{p^{-2}[m]^2_{p,q}}{qR_{p,q}(m,\beta)T_{p,q}(m,2)}x+\frac{\alpha}{R_{p,q}(m,\beta)}} \left(\frac{p^{-2}[m]^2_{p,q}}{qR_{p,q}(m,\beta)T_{p,q}(m,2)}x+\frac{\alpha}{R_{p,q}(m,\beta)}-u\right)g''(u)du\right| \\
&\le \frac{\|g''\|_B}{2}H^{\alpha,\beta}_{m,p,q}((t-x)^2,x)+\frac{\|g''\|_B}{2}\left(\left(\frac{p^{-2}[m]^2_{p,q}}{qR_{p,q}(m,\beta)T_{p,q}(m,2)}-1\right)+\frac{\alpha}{R_{p,q}(m,\beta)}\right)^2 \\
&\le \frac{\|g''\|_B}{2}\left\{\left(\frac{2(1-p^{-2}q^3)}{q^4}+\frac{288(\alpha+\beta+1)^2[m]_{p,q}}{q^4T_{p,q}(m,3)}\right)(x^2+x)+\frac{\alpha^2}{\left(R_{p,q}(m,\beta)\right)^2}\right\} \\
&+\frac{\|g''\|_B}{2}\left\{\left(\frac{p^{-4}[m]^4_{p,q}}{\left(qR_{p,q}(m,\beta)T_{p,q}(m,2)\right)^2}-\frac{2p^{-2}q[m]^2_{p,q}\left([m]_{p,q}+\beta\right)[m-2]_{p,q}}{\left(qR_{p,q}(m,\beta)T_{p,q}(m,2)\right)^2}\right.\right. \\
&\left.-\frac{q^2\left([m]_{p,q}+\beta\right)^2[m-2]^2_{p,q}}{\left(qR_{p,q}(m,\beta)T_{p,q}(m,2)\right)^2}\right)x^2+\frac{2\alpha\left(p^{-2}[m]^2_{p,q}-q\left([m]_{p,q}+\beta\right)[m-2]_{p,q}\right)}{qR^2_{p,q}(m,\beta)T_{p,q}(m,2)}x \\
&\left.+\frac{\alpha^2}{\left(R_{p,q}(m,\beta)\right)^2}\right\} \\
&\le \left\{\left(\frac{2(1-p^{-2}q^3)}{q^4}+\frac{332(\alpha+\beta+1)^2}{q^4T_{p,q}(m,2)}\right)(x^2+x)+\frac{\alpha^2}{\left(R_{p,q}(m,\beta)\right)^2}\right\}\|g''\|_B.
\end{aligned}$$

Finally, the proof of Lemma 4 is completed.

Theorem 1 Let $(p_m),(q_m)\subset(0,1)$ be two sequences with $0<q_m<p_m\le 1$ such that $p_m\to 1, q_m\to 1$ as $m\to\infty$. Then for every $m>3$ and $g\in C_B[0,\infty)$, we have the below inequality

$$\left|H^{\alpha,\beta}_{m,p_m,q_m}(g,x)-g(x)\right|\le 2Cw_2\left(g,\sqrt{\zeta^{\alpha,\beta}_{m,p_m,q_m}(x)}\right)+w\left(g,\eta^{\alpha,\beta}_{m,p_m,q_m}(x)\right),$$

Where $\eta^{\alpha,\beta}_{m,p_m,q_m}(x)=\left(\frac{{p_m}^{-2}[m]^2_{p_m,q_m}}{q_mR_{p_m,q_m}(m,\beta)T_{p_m,q_m}(m,2)}-1\right)x+\frac{\alpha}{R_{p_m,q_m}(m,\beta)}$.

Proof. Based on (10), for any $g\in W^2_\infty$, we obtain the inequality

$$\left|H^{\alpha,\beta}_{m,p_m,q_m}(g,x)-g(x)\right| \le \left|\overline{H}^{\alpha,\beta}_{m,p_m,q_m}(g-f,x)-(g-f)(x)+H^{\alpha,\beta}_{m,p_m,q_m}(f,x)-f(x)\right|$$

$$+\left|g\left(\frac{p_m{}^{-2}[m]_{p_m,q_m}^2 x}{q_m R_{p_m,q_m}(m,\beta)T_{p_m,q_m}(m,2)}+\frac{\alpha}{R_{p_m,q_m}(m,\beta)}\right)-g(x)\right|.$$

From Lemma 4, we get

$$\begin{aligned}\left|H_{m,p_m,q_m}^{\alpha,\beta}(g,x)-g(x)\right| &\leq 2\|g-f\|_B+\zeta_{m,p_m,q_m}^{\alpha,\beta}(x)\|f''\|_B \\ &+\left|g\left(\frac{p_m{}^{-2}[m]_{p_m,q_m}^2 x}{q_m R_{p_m,q_m}(m,\beta)T_{p_m,q_m}(m,2)}+\frac{\alpha}{R_{p_m,q_m}(m,\beta)}\right)-g(x)\right|.\end{aligned}$$

As a result of the equality (6), we have the inequality

$$\left|H_{m,p_m,q_m}^{\alpha,\beta}(g,x)-g(x)\right| \leq 2\|g-f\|_B+\zeta_{m,p_m,q_m}^{\alpha,\beta}(x)\|f''\|_B+w\left(g,\eta_{m,p_m,q_m}^{\alpha,\beta}(x)\right).$$

Taking the infimum over $g \in W_\infty^2$ on the right-hand side of the above inequality and then using the inequality (8), we get the desired result.

Theorem 2 Let $(p_m),(q_m) \subset (0,1)$ be two sequences with $0<q_m<p_m \leq 1$ such that $p_m \to 1,\ q_m \to 1$ as $m \to \infty$. Then $g \in C_\sigma^*[0,\infty)$, we have

$$\lim_{m\to\infty}\left\|H_{m,p_m,q_m}^{\alpha,\beta}(g,x)-g(x)\right\|_\sigma=0.$$

Proof. From Lemma 1, it is obvious that $\left\|H_{m,p_m,q_m}^{\alpha,\beta}(e_0,x)-e_0\right\|_\sigma=0$. Because

$\left|\frac{p_m{}^{-2}[m]_{p_m,q_m}^2 x}{q_m R_{p_m,q_m}(m,\beta)T_{p_m,q_m}(m,2)}+\frac{\alpha}{R_{p_m,q_m}(m,\beta)}-x\right| \leq (x+1)o(1)$ and $\frac{1+x}{1+x^2}$ is positive and it is bounded from above for each $x \geq 0$, we get

$$\left\|H_{m,p_m,q_m}^{\alpha,\beta}(e_1,x)-e_1\right\|_\sigma \leq \frac{1+x}{1+x^2}o(1).$$

And then $\lim_{m\to\infty}\left\|H_{m,p_m,q_m}^{\alpha,\beta}(e_1,x)-e_1(x)\right\|_\sigma=0.$

Similarly for every $m > 3$, we can write

$$\begin{aligned}\left\|H_{m,p_m,q_m}^{\alpha,\beta}(e_2,x)-e_2(x)\right\|_\sigma &= \sup_{x\in[0,\infty)}\left\{\frac{\left|\frac{p_m{}^{-3}[m]_{p_m,q_m}^4 x^2}{q_m^4\left(R_{p_m,q_m}(m,\beta)\right)^2 T_{p_m,q_m}(m,3)}\right.}{1+x^2}\right. \\ &+\frac{\left\{\frac{p_m{}^{-5}[2]_{p_m,q_m}[m]_{p_m,q_m}^3 x^2}{q_m^4\left(R_{p_m,q_m}(m,\beta)\right)^2 T_{p_m,q_m}(m,3)}+\frac{2\alpha p_m{}^{-3}[m]_{p_m,q_m}^2}{q_m^2\left(R_{p_m,q_m}(m,\beta)\right)^2 T_{p_m,q_m}(m,3)}\right\}x}{1+x^2} \\ &\left.+\frac{\left.\frac{\alpha^2}{\left(R_{p_m,q_m}(m,\beta)\right)^2}-x^2\right|}{1+x^2}\right\}\end{aligned}$$

$$\leq \sup_{x\in[0,\infty)} \frac{1+x+x^2}{1+x^2} o(1),$$

and we get $\lim_{m\to\infty} \left\| H^{\alpha,\beta}_{m,p_m,q_m}(e_2,x) - e_2(x) \right\|_\sigma = 0$. Therefore, by using A. D. Gadzhiev.s Theorem in Gadzhiev (1976), we obtain Theorem 2's result.

Lemma 5 Let $g \in C_\sigma[0,\infty)$, $(p_m),(q_m) \subset (0,1)$ be two sequences with $0 < q_m < p_m \leq 1$ such that $p_m \to 1, q_m \to 1$ as $m \to \infty$ and $w_{[0,d+1]}(g,\delta)$ be its modulus of continuity on the finite interval $[0,d+1]$ $d > 0$. Then for every $m > 3$, there exists a constant $C > 0$ such that the inequality holds

$$\left\| H^{\alpha,\beta}_{m,p_m,q_m}(g,x) - g(x) \right\|_{C[0,d]} \leq C\left\{(d+1)^2 \xi^{\alpha,\beta}_{m,p_m,q_m}(d) + w_{[0,d+1]}\left(g, \sqrt{\xi^{\alpha,\beta}_{m,p_m,q_m}(d)}\right)\right\},$$

where

$$\xi^{\alpha,\beta}_{m,p_m,q_m}(d) = \left(\frac{2(1-p_m^{-2}q_m^3)}{q_m^4} + \frac{288(\alpha+\beta+1)^2[m]_{p_m,q_m}}{q_m^4 T_{p_m,q_m}(m,3)}\right)(d^2+d) + \frac{\alpha^2}{\left(R_{p_m,q_m}(m,\beta)\right)^2}.$$

Proof. Let $x \in [0,d]$ and $t > d+1$. Since $t - x > 1$, we have

$$\begin{aligned} |g(t)-g(x)| &\leq M_g(2+t^2+x^2) \\ &\leq 3M_g(1+d)^2(t-x)^2. \end{aligned} \tag{11}$$

Let $x \in [0,d]$ and $t < d+1$ and $\delta > 0$. Then we have

$$|g(t)-g(x)| \leq \left(1+\frac{|t-x|}{\delta}\right) w_{[0,d+1]}(g,\delta). \tag{12}$$

With the help of (11) and (3.12), we can write

$$|g(t)-g(x)| \leq 3M_g(1+d)^2(t-x)^2 + \left(1+\frac{|t-x|}{\delta}\right) w_{[0,d+1]}(g,\delta).$$

Then, using Lemma 2 and Cauchy-Schwarz's inequality, we get the following inequalities

$$\begin{aligned} \left|H^{\alpha,\beta}_{m,p_m,q_m}(g,x) - g(x)\right| &\leq 3M_g(1+d)^2 H^{\alpha,\beta}_{m,p_m,q_m}((t-x)^2,x) \\ &\quad + w_{[0,d+1]}(g,\delta)\left[1+\frac{1}{\delta}\left(H^{\alpha,\beta}_{m,p_m,q_m}((t-x)^2,x)\right)^{1/2}\right] \\ &\leq 3M_g(1+d)^2 \xi^{\alpha,\beta}_{m,p_m,q_m}(x) + w_{[0,d+1]}(g,\delta)\left[1+\frac{1}{\delta}\left(\xi^{\alpha,\beta}_{m,p_m,q_m}(x)\right)^{1/2}\right], \end{aligned}$$

where

$$\xi^{\alpha,\beta}_{m,p_m,q_m}(x) = \left(\frac{2(1-p_m^{-2}q_m^3)}{q_m^4} + \frac{288(\alpha+\beta+1)^2[m]_{p_m,q_m}}{q_m^4 T_{p_m,q_m}(m,3)}\right)(x^2+x) + \frac{\alpha^2}{\left(R_{p_m,q_m}(m,\beta)\right)^2}$$

Setting

$$\delta^2 := \xi^{\alpha,\beta}_{m,p_m,q_m}(d) = \left(\frac{2(1-p_m^{-2}q_m^3)}{q_m^4} + \frac{288(\alpha+\beta+1)^2[m]_{p_m,q_m}}{q_m^4 T_{p_m,q_m}(m,3)}\right)(d^2+d) + \frac{\alpha^2}{\left(R_{p_m,q_m}(m,\beta)\right)^2}$$

and $C = \min\{3M_g, 2\}$. Therefore, the proof of Lemma 5 is finished.

Theorem 3 Let $\lambda > 0, (p_m), (q_m) \subset (0,1)$ be two sequences with $0 < q_m < p_m \leq 1$ such that $p_m \to 1$, $q_m \to 1$ as $m \to \infty$ and $g \in C_\sigma^*[0,\infty)$. Then we have

$$\lim_{m\to\infty} \sup_{x\geq 0} \frac{\left|H^{\alpha,\beta}_{m,p_m,q_m}(g,x) - g(x)\right|}{1+x^{2+\lambda}} = 0.$$

Proof. For $\lambda > 0, g \in C_\sigma^*[0,\infty)$ and $b > 1$, the following inequality is ensured

$$\begin{aligned}
\sup_{x\geq 0} \frac{\left|H^{\alpha,\beta}_{m,p_m,q_m}(g,x) - g(x)\right|}{1+x^{2+\lambda}} &\leq \sup_{0\leq x<d} \frac{\left|H^{\alpha,\beta}_{m,p_m,q_m}(g,x) - g(x)\right|}{1+x^{2+\lambda}} + \sup_{d\leq x} \frac{\left|H^{\alpha,\beta}_{m,p_m,q_m}(g,x) - g(x)\right|}{1+x^{2+\lambda}} \\
&\leq \left\|H^{\alpha,\beta}_{m,p_m,q_m}(g,x) - g(x)\right\|_{C[0,d]} + \sup_{d\leq x} \frac{\left|H^{\alpha,\beta}_{m,p_m,q_m}(g,x) - g(x)\right|}{1+x^{2}} \\
&\leq \left\|H^{\alpha,\beta}_{m,p_m,q_m}(g,x) - g(x)\right\|_{C[0,d]} + \left\|H^{\alpha,\beta}_{m,p_m,q_m}(g,x) - g(x)\right\|_{\sigma}.
\end{aligned}$$

Using Lemma 5 and Theorem 2, the proof of Theorem 3 is provided.

CONFLICT OF INTEREST

The authors declare no conflict of interest.

REFERENCES

Acar, T., Aral, A., & Mohiuddine, S. A. (2016). On Kantorovich modication of *(p, q)*-Baskakov operators. *Journal of Inequalities and Applications*, *2016*, 98. doi:10.1186/s13660-016-1045-9

Acar, T., Aral A., & Mohiuddine, S. A. (2018). Approximation by Bivariate *(p, q)*-Bernstein-Kantorovich operators. *Iranian Journal of Science and Technology, Transactions A: Science*, *42*(2), 655-662. doi:10.1007/s40995-016-0045-4

Aral, A., Gupta, V., & Agarwal, R. P. (2013). *Applications of q-calculus in operator theory*. Springer, New York. doi:10.1007/978-1-4614-6946-9

Cai, Q-B., Sofyalıoglu, M., Kanat, K., & Çekim, B. (2021). Some approximation results for the new modification of Bernstein-Beta operators *AIMS Mathematics*, *7*(2), 1831-1844. doi:10.3934/math.2022105

De Sole, A., & Kac, V. G. (2005). On integral representations of q-gamma and q-beta functions. *Atti Accad. Naz. Lincei Cl. Sci. Fis. Mat. Natur. Rend. Lincei Mat. Appl.*, *16*(1), 11-29.

Dinlemez, Ü., Yüksel, İ., & Altın, B. (2014). A note on the approximation by the q-hybrid summation integral type operators. *Taiwanese Journal of Mathematics*, *18*(3), 781-792.

Doğru, O., & Gupta, V. (2005). Monotonicity and the asymptotic estimate of Bleimann Butzer and Hahn operators based on q -integers. *Georgian Mathematical Journal*, *12*(3), 415-422.

Doğru, O., & Gupta, V. (2006). Korovkin-type approximation properties of bivariate q-Meyer-König and Zeller operators. *Calcolo*, *43*(1), 51-63. doi:10.1007/s10092-006-0114-8

Gadzhiev, A. D. (1976). Theorems of the type of P. P. Korovkin type theorems. *Matematicheskie Zametki*, *20*(5), 781-786. English Translation: *Math. Notes*, *20*(5/6), 996-998.

Gupta, V., & Heping, W. (2008). The rate of convergence of q-Durrmeyer operators for 0<q<1. *Mathematical Methods in the Applied Sciences*, *31*(16), 1946-1955. doi:10.1002/mma.1012

Gupta, V., & Aral, A. (2010). Convergence of the q-analogue of Szász-beta operators. *Applied Mathematics and Computation*, *216*(2), 374-380. doi:10.1016/j.amc.2010.01.018

Gupta, V., & Karsli, H. (2012). Some approximation properties by q-Szász-Mirakyan-Baskakov-Stancu operators. *Lobachevskii Journal of Mathematics*, *33*(2), 175-182. doi:10.1134/S1995080212020138

Gupta, V. (2018). *(p, q)*-Szász-Mirakyan-Baskakov Operators. *Complex Analysis and Operator Theory*, 12, 17-25. doi:10.1007/s11785-015-0521-4

Jackson, F. H. (1910). On q-Definite Integrals. *The Quarterly Journal of Pure and Applied Mathematics*, *41*(15), 193-203.

Kac, V. G., & Cheung, P. (2002). *Quantum Calculus*. Part of the Universitext book series, Springer-Verlag, New York. doi:10.1007/978-1-4613-0071-7

Kanat, K., & Sofyalıoğlu, M. (2018). Approximation by *(p, q)*-Lupaş–Schurer–Kantorovich operators. *Journal of Inequalities and Applications*, *2018*, 263. doi:10.1186/s13660-018-1858-9

Kanat, K., & Sofyalıoğlu, M. (2021). On Stancu type Szász-Mirakyan-Durrmeyer Operators Preserving exp(2ax), a > 0. *Gazi University Journal of Science*, *34*(1), 196-209. doi:10.35378/gujs.691419

Koelink, H. T., & Koornwinder, T. H. (1990). q-special functions, a tutorial. In: M. Gerstenhaber, & J. Stasheff (Eds.) Deformation Theory and Quantum Groups with Applications to Mathematical Physics (Proceedings of an AMS-IMS-SIAM 1990), *Contemporary Mathematics*, *134*, 141-142.

Lupaş, A. (1987). A q-analogue of the Bernstein operator. In: *Seminar on numerical and statistical calculus, University of Cluj-Napoca*, 9, 85-92.

Mursaleen, M., Ansari, K. J., & Khan, A. (2015a). On *(p, q)*-analogue of Bernstein operators. *Applied Mathematics and Computation*, *266*, 874-882. doi:10.1016/j.amc.2015.04.090

Mursaleen, M., Ansari, K. J., & Khan, A. (2015b). Some Approximation Results by *(p, q)*-analogue of Bernstein-Stancu operators. *Applied Mathematics and Computation*, *264*, 392-402. doi:10.1016/j.amc.2015.03.135

Mursaleen, M., Nasiuzzaman, Md., & Nurgali, A. (2015c). Some approximation results on Bernstein-Schurer operators dened by *(p, q)*-integers. *Journal of Inequalities and Applications*, *2015*, 249. doi:10.1186/s13660-015-0767-4

Phillips, G. M. (1997). Bernstein polynomials based on the q-integers. *Annals of Numerical Mathematics*, *4*(1-4), 511-518.

Sahai, V., & Yadav, S. (2007). Representations of two parameter quantum algebras and *(p, q)*-special functions. *Journal of Mathematical Analysis and Applications*, *335*(1), 268-279. doi:10.1016/j.jmaa.2007.01.072

Sofyalıoğlu, M., Kanat, K., & Çekim, B. (2021). Parametric generalization of the Meyer-König-Zeller operators. *Chaos, Solitons & Fractals*, *152*, 111417. doi:10.1016/j.chaos.2021.111417

Yüksel, İ. (2013). Direct results on the q-mixed summation integral type operators. *J. Applied Functional Analysis*, *8*(2), 235-245.

Research Article / Araştırma Makalesi GU J Sci, Part A, 9(1): 12-24 (2022) https://doi.org/10.54287/gujsa.1074379

Gazi University
Journal of Science
PART A: ENGINEERING AND INNOVATION
http://dergipark.org.tr/gujsa

Effect of Equipment Component Generic Frequency Data on Probability of Failure Calculations for Risk-Based Inspection

Ibrahim TUKENMEZ[1*], Huseyin Baran AKINBINGOL[1]

[1]*Gazi University Faculty of Engineering, Ankara, Turkey*

Keywords

Major Accident Scenario Frequency

Probability of Failure

Risk Based Inspection

Corrosion

Abstract

A software was developed to use equipment component frequency data specific to the facility or provided from different sources in lost event probability calculations for risk-based inspection. Corrosion causes equipment aging and loss events in which hazardous substances are released uncontrollably. The API RP 581 Recommended Practise of the American Petroleum Institute is widely used in the calculation of corrosion-based loss event risks for static pressure equipment such as atmospheric tanks, heat exchangers, columns, reactors, and used for basis of the developed software. In API RP 581, the risk of loss event is defined as the product of the probability of failure and the severity of consequence. Equipment component generic failure frequencies are a variable at the probability of failure calculation. Current software use only equipment component generic failure frequencies given at API RP 581. For this reason, establishment-specific equipment component failure frequency data or data that can be obtained from other sources cannot be used. To solve this problem, a software based on API RP 581 methodology has been developed and provided with the opportunity for the user to enter equipment component failure frequency data from different sources. The findings showed that when using data from different literature sources, there are different results up to 1491% in the probability of failures. Since the increase in the probability of the failures will increase the risk, that creates results such as pulling the equipment inspection dates forward, performing more effective and therefore more costly inspections, increasing the precautions and costs to be taken. Therefore, software which are based on API RP 581 methodology should be developed in such a way that different generic frequency data can be used.

Cite

Tukenmez, I., & Akinbingol, H. B. (2022). Effect of Equipment Component Generic Frequency Data on Probability of Failure Calculations for Risk-Based Inspection. *GU J Sci, Part A*, *9*(1), 12-24.

Author ID (ORCID Number)

I. Tukenmez, 0000-0003-3669-2160
H. B. Akinbingol, 0000-0002-4020-6359

Article Process	
Submission Date	16.02.2022
Revision Date	09.03.2022
Accepted Date	18.03.2022
Published Date	25.03.2022

1. INTRODUCTION

According to the Regulation on Prevention of Major Industrial Accidents And Lessening Their Adverse Impacts (2019) major industrial accident is defined as a major spread, fire or explosion event during the operation of an establishment caused by one or more dangerous substances. Those events may cause immediate or later serious danger to human and/or environmental health inside or outside the establishment, resulting from uncontrolled developments (URL1, 2019).

Corrosion is one of the main causes of major industrial accidents (Wood et al., 2013; Baybutt, 2015). Loss of containment due to disruption of the integrity of the equipment component may result not only from the corrosive properties of hazardous materials, but also from the properties of the material from which the equipment is manufactured, operating environment, operating conditions, or their interaction (API RP 581, 2016).

*Corresponding Author, e-mail: ibrahim.tukenmez@gazi.edu.tr

Concepts such as the prevention of process safety in major industrial accidents caused by corrosion and aging have become a subject of process safety in various legislations around the world. For the manufacturers and users of these equipment, starting from the design, the inspection, maintenance and repairs, evaluations and various reasons in terms of the number, variety, costs, effectiveness and focus of the equipment have revealed the need for a risk-based corrosion management strategy.

There are guides, standards, codes and similar various documents have been published by both non-profit organizations and various private sector organizations on corrosion damage mechanisms, estimation of major industrial accident risk, development of risk-based inspection (RBI) methodology and risk management. ASME PCC-3:2007, EN 16991:2016, DNV-RP-G101:2002, EEMUA206:2006, EEMUA 159:2017 and API RP 581:2016 are the most widely known among these documents (EN 16991, ASME-PCC-3, EEMUA 206, EEMUA 159, DNV-RP-G101). There are different qualitative and quantitative approaches in the published documents for the estimation of corrosion based damage mechanisms' risks. Documents are being updated due to reasons such as the need to evaluate the effects of various variables such as the chemical substance, equipment and components, corrosion mechanism, inspection and control techniques, differences in management system evaluation in the estimation of risk.

The American Petroleum Institute has two recommended practices which are API RP 580 and API RP 581, for guidelines on risk-based inspection. Since the 1990s, the issue of risk-based inspection on static pressure equipment has come to the fore in chemical processes where toxic, flammable and explosive dangerous chemicals are processed and stored, especially in petroleum refineries. With the sponsorship of some of the leading international companies in the refining, petrochemical and chemical industries, first the American Petroleum Institute (API) published the Basic Resource Document, which revealed the risk-based inspection (RBI) methodology, and then the risk-based inspection recommended practice in 2000 (Revie, 2015)

API RP 580 sets out the basic requirements for risk-based inspection, but does not go into methodology and details. API RP 581 allows detailed quantitative analyzes to be made on different corrosion-based damage mechanisms with its unique formulas, tables and graphics (API RP 581). For this reason, it is widely used all over the world compared to other standards, guides or norms and contributes to the development of software.

However, there are some problems and limitations both in the API RP 581 recommended practice and software which are based on API RP 581. One of them is to use only the equipment component failure frequency values based on corrosion damage mechanisms in equipment components given in the API RP 581 instead of the facility's own data or the values given in different references.

There are various studies in the literature regarding the effects of differences in generic equipment component failure frequency values (GFF) on risk in terms of equipment components. Considering the differences between failure frequency data in industry and the need to improve data quality, Keeley et al. (2011) conducted a study on the work program conducted by the UK Health and Safety Laboratory (HSL), which brought together and updated existing failure frequency data sources and reviewed new sources that were not previously available (Keeley et al., 2011).

Pittiglio et al. (2014) found that in the process industries, decisions such as equipment inspection, maintenance, and change management have become more "risk-based" over time, but the differences in the failure frequency data used in risk calculations and their differences from major systematic studies in the 1960s-1970s stated that new studies are necessary for these reasons (Pittiglio et al., 2014).

In this study it' s aimed to reveal the effect of equipment component generic failure frequency (GFF) data on probability of failure (POF) calculations based on API RP 581 methodology. To do that, a flexible software is developed which has capability of data input from user. That kind of software flexibility provides opportunity to use establishment specific and/or literature GFF values for the user. The developed software calculates POF value using GFF values given at API RP 581 as default and at the same time another POF can be calculated if the user inputs another GFF value.

2. MATERIAL AND METHOD

2.1. API RP 581 Risk-Based Inspection Methodology Overview

API RP 581 risk-based inspection is a method in which the frequency values of the loss of containment that may occur due to corrosion of pressure equipment and the areal and financial severity of the results of fire, explosion or toxic release that may occur as a result of loss of containment are evaluated as the two basic elements of risk (Figure 1).

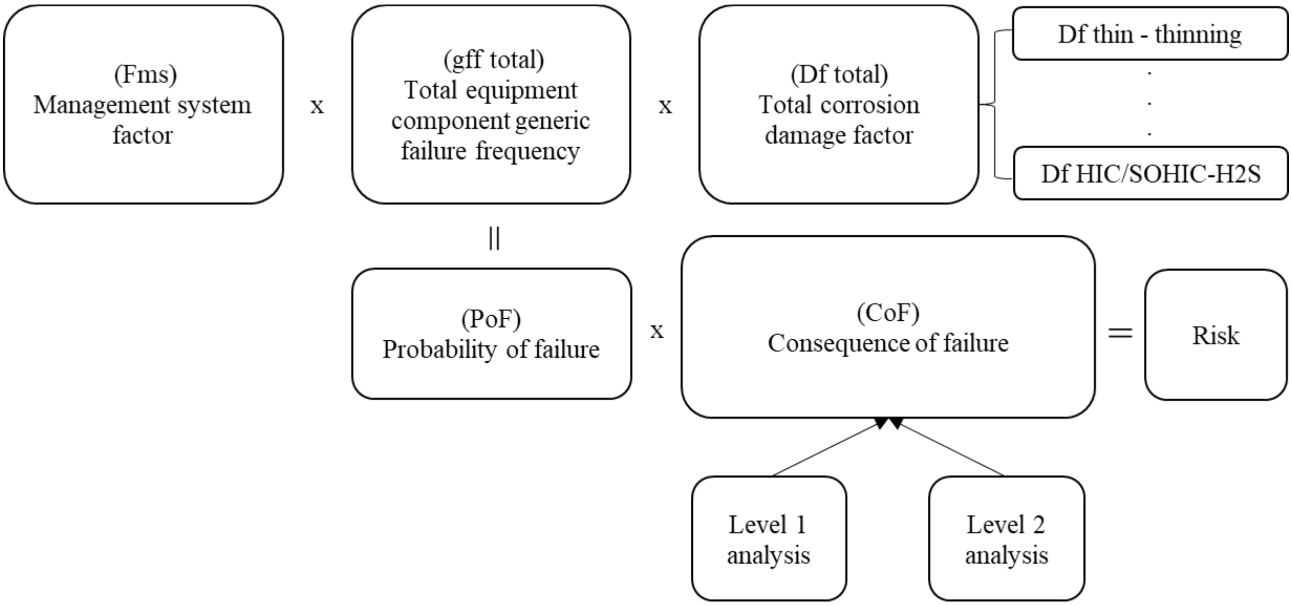

Figure 1. *Risk estimation general components for risk-based inspection according to API RP 581*

It is expressed as the annual potential occurrence frequency (Pf (t) since it depends on time) of different degrees of failure frequency that occur in the equipment due to the corrosion mechanism depending on the hazardous chemical substance in the equipment, and the working conditions, and the working environment. The expression "failure" used by API RP 581 means "loss of containment/integrity" that causes loss events. Failure sizes are represented by representative hole diameters of a given diameter in varying range (Table 1). Generic failure frequency (GFF) data for equipment component types can not be used alone for POF calculations without corrosion mechanism and management system adjustment factors because those obtained GFF values from industry are not specific to the failure mechanism and establishment. Some of the GFF values given for equipment components in API RP 581 are given in Table 2.

A correction is made in the POF calculation by multiplying the GFF values by the management system factor (F_{ms}) of the establishment where the risk is evaluated and the sum of the time-dependent damage factors (Df(t)) of the damage mechanisms caused by the corrosion in the equipment. Accordingly, PoF calculation is made according to equation 1.

$$P_f(t) = GFF_{total}\ x\ F_{ms}\ x\ D_f(t) \quad (1)$$

Correction factors with a value greater than 1.0 will increase the POF and those with a value less than 1.0 will decrease it. Both correction factors are always positive numbers.

2.1.1. Equipment Component GFF Values in API RP 581

In API RPI 581, GFF values are differentiated according to both the equipment and its component and the representative hole diameters of a certain diameter in a geometrically varying range of damage size. In this regard, different GFF values in each different categorical equipment component are given as different numerical values according to the damage size in 4 different hole diameters. These diameters and some of the equipment component GFF values are given in Table 1 (API RP 581).

***Table 1.** Hole sizes used in level 1 and 2 consequence analysis (COF) in API RP 581*

Release Hole Number	Release Hole Type	Range of Release Hole Diameter (mm)	Release Hole Diameter, d_n (mm)
1	Small	0 - 6.4	d_1 = 6.4
2	Medium	>6.4 to 51	d_2 = 25; d_2 = minimum [D,25]
3	Large	>51 to 152	d_3 = 102; d_3 = minimum [D,102]
4	Rupture	>152	d_4 = minimum [D,406]

***Table 2.** GFF values for the some of the equipment components given in API RP 581*

Equipment Type	Component Type	Small Hole GFF	Medium Hole GFF	Large Hole GFF	Rupture GFF	GFF Total (failure/year)
Compressor	Compressor R	8.00E-06	2.00E-05	2.00E-06	6.00E-07	3.06E-05
Heat Exchanger	ID SS	8.00E-06	2.00E-05	2.00E-06	6.00E-07	3.06E-05
	ID TS	8.00E-06	2.00E-05	2.00E-06	6.00E-07	3.06E-05
Pipe	Pipe-1	2.80E-05	0	0	2.60E-06	3.06E-05
	Pipe-2	2.80E-05	0	0	2.60E-06	3.06E-05
Pump	Pump2S	8.00E-06	2.00E-05	2.00E-06	6.00E-07	3.06E-05
Atmospheric Storage Tank	Tank bottom	7.20E-04	0	0	2.00E-06	7.22E-04
	Shell-1-10	7.00E-05	2.50E-05	5.00E-06	1.00E-07	1.00E-04
Vessel/FinFan	Codrum	8.00E-06	2.00E-05	2.00E-06	6.00E-07	3.06E-05
	Drum	8.00E-06	2.00E-05	2.00E-06	6.00E-07	3.06E-05
	FinFan	8.00E-06	2.00E-05	2.00E-06	6.00E-07	3.06E-05
	Reactor	8.00E-06	2.00E-05	2.00E-06	6.00E-07	3.06E-05

2.1.2. Equipment Component GFF Values in Other Literature

Within the scope of Seveso II Directive studies in Europe, the Purple Book (CPR 18E, 2005) published by the Ministry of Housing, Spatial Planning and the Environment to guide quantitative risk assessment includes the release frequencies of hazardous materials for equipment. The release frequency data was based on various government-sponsored projects, expert opinions and other known sources, and sources were addressed for each equipment type. The events that cause the release frequency are named as loss of containment. Loss events are categorized with the G lettering. According to this;

G.1: Sudden release of entire inventory

G.2: Discharge of the entire inventory within 10 minutes by continuous release at a constant release rate

G.3: Continuous release through a hole with an effective diameter of 10 mm

As an example, the release frequencies given in the Purple Book on constant pressure vessels on an annual basis are given in Table 3.

***Table 3.** Pressure vessel failure frequency examples from Purple Book*

Equipment	G1.	G2.	G3.
Pressure vessel	5×10^{-7}	5×10^{-7}	1×10^{-5}
Process vessel	5×10^{-6}	5×10^{-6}	5×10^{-4}
Reactor vessel	5×10^{-6}	5×10^{-6}	5×10^{-4}

Quantitative risk assessment data has been provided to the chemical process industries by the American Center for Chemical Safety (CCPS) since the 1980s. CCPS published the “CCPS Guidelines for Process Equipment Reliability Data” in 1989 and “Guidelines for Improving Plant Reliability through Data Collection and Analysis” in 1998. Subsequent enhancements in this information-gathering effort have allowed the creation of the Process Equipment Reliability Database (PERD), which provides deeper and more specific analysis of equipment availability, reliability, design improvements, maintenance strategies, and life-cycle cost determination (AIChE PERD, 2020).

In the Guidelines For Initiating Events And Independent Protection Layers In Layer of Protection Analysis book, the frequency of catastrophic integrity loss for pressure vessels is stated as 1 x 10^{-5} per year (CCPS, 2014).

The International Oil and Gas Producers Association (IOGP) publishes the “process release frequencies” report at regular intervals. The current data presented in the 2019 IOGP Process release frequencies report is based on the analysis of data from the United Kingdom Health and Safety Executive (HSE) Hydrocarbon Release Database (HCRD) from 1992 to 2015. The data sheets to be used for the equipment are grouped separately from each other in accordance with the explanations above, unlike API RP 581. As an example, generic failure frequency data for process (pressurized) equipment is given in Table 4 (IOGP, 2019).

Table 4. *IOGP process release frequencies report process equipment leak frequency data*

Hole Diameter Range (mm)	Inlets 50 to 150 mm Diameter	Inlets >150 mm Diameter
1 to 3	5.0E-04	5.0E-04
3 to 10	2.6E-04	2.6E-04
10 to 50	1.4E-04	1.4E-05
50 to 150	7.4E-05	3.8E-05
>150	---	3.6E-05
Total	9.8E-04	9.8E-04

Det Norske Veritas (DNV) process release frequency data are also frequently used in the industry. Like IOGP, DNV data are based on HCRD and some other data sources. DNV, derives data from HCRD data, but with a different equation than IOGP. There is derived equation is used in the DNV Leak software to generate the release frequencies for the lost event. The release frequency data of the process vessel calculated by the software are given as an example in Table 5 (DNV, 2013).

Table 5. *DNV Leak process vessel release frequency data*

Proses vessel Frequency data				
Equipment Size	Category	Total	Full Pressure	Zero Pressure
	3 - 10 mm	5.946E-04	4.093E-04	1.393E-04
	10 - 50 mm	4.379E-04	2.236E-04	1.408E-04
	50 - 150 mm	1.652E-04	6.181E-05	7.316E-05
	> 150 mm	2.736E-04	5.930E-05	2.977E-04
	Total	2.360E-03	1.540E-03	8.110E-04

2.1.3. POF Algorithm and Calculation

In this study, like as other existing software used in industrial applications, API RP 581 RBI methodology is followed for the POF calculation and algorithm is given in Figure 2.

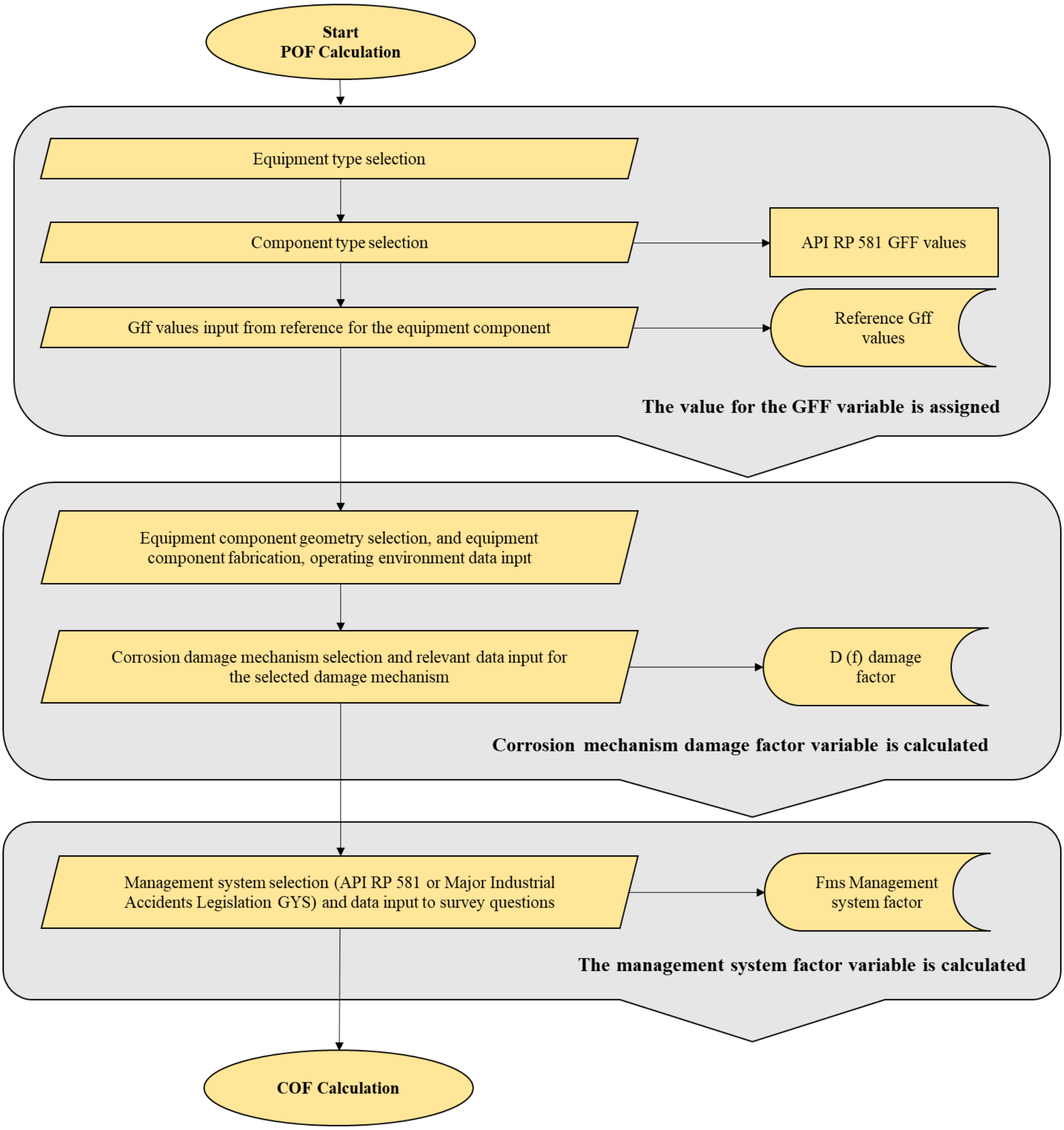

Figure 2. *POF calculation algorithm*

3. CASE STUDY

The case study is RBI calculation on a drum. Operating temperature, T, is 49˚C and pressure, P, 0.696 MPa. In drum the fluid is a mixture of propane and butane with 0.11% H_2S. Operating conditions allow aqueous conditions, general corrosion is inspected. Measured corrosion rate of 0.29 mm per year. Also, stress corrosion cracking caused by wet H_2S is possible with a susceptibility of Low. B effectiveness level inspection results on 04.04.2003 revealed some general corrosion and thickness is measured as 19.05 mm. There is no history of inspection for wet H_2S cracking. The management system is evaluated and was found to be 0.5. Mechanical design parameters of the drum, operating conditions, some properties related to the fluid it limits and inspection values are given in Table 6, 7 and 8.

The values of the case studies were entered into the software developed according to the formulas and tables in the sections on POF calculation in the current edition of API RP 581 in 2016. Since the features of the software such as management systems evaluation and result analysis are out of the scope of this study, only the screenshots of the data inputs of the user interface of the developed software related to this study are given in Figures 3, 4 and 5. The user interface for equipment component data of the developed software screenshot given in Figure 3. The user selects the equipment and component type which is intended to be evaluated for RBI study and the GFF values given at API RP 581 are automatically assigned to the calculations at backend of the software which are stored and called from Microsoft SQL Database. If the user wants to use other GFF value from other references than API RP 581 those data shall be entered by manually. For the calculation POF and Risk the user inputs are categorized as equipment component fabrication values such as yield / tensile strength, allowable stress load; component geometry such as cylindirical (CYL), inside diameter, and working environment such as working temperature which are all given at Table 6. Those data shall be entered by manually from the user. The user interface for corrosion mechanism data of the developed software screenshot given in Figure 4. The user interface for consequence of failure (COF) and risk evaluation at Figure 5, which are all user input data and leaved as constant values just for this study.

Table 6. *Drum design, operating conditions, fluid-related data*

Design data		**Equipment Component type**	Cylindrical shell-CYL
Design code	EN ISO	Inside diameter, mm	2479.675
Material of construction	Carbon steel	Length, mm	9144
Yield / Tensile strength, MPa	205 / 380	Volume, m^3	44.136
Allowable stress load, MPa	94.8	**Process fluid**	
Weld joint efficiency (0.7-1)	0.85	Name	mixture of propane and butane
Post weld heat treatment	Yes	Liquid ratio (0-1)	0.5
Design temperature, °C	232	Gas ratio (0-1)	0.5
Design pressure, MPa	1.138	Type	Type 0
Furnished thickness, mm	20.637	Phase in the equipment	2 phase (liquid-gas)
Corrosion allowance, mm	3.175	Molecular weight, MA, kg/kmol	51
Cladding/weld overlay	-	Liquid phase density, p_l, kg/m^3	538.379
Thickness of weld cap, mm	0	Gas phase density, p_g, kg/m^3	5.97
Equipment type	Pressure vessel	Normal boiling point, °C	-21
Component type	Drum	Physical state outside	Gas
Fabrication date	1.01.1972	Autoignition temprature, °C	369
Service date	1.01.1972	Ideal Gas Specific Heat Capacity Ratio, k (unitless)	1.13

Table 7. *Thinning inspection results*

D_f thin (General and local D_f) Inspection 1		
Date	04.04.2003	
Damage mechanism	D_f ^{Thin}	
Effectiveness	D_f ^{thin} – Inside - B: Usually effective	
Measured thickness, t_{rdi}, mm	19.05	
Corrosion rate, mm/year	Measured	0.29
Corrosion Rate Confidence Levels	High Confidence	3
Thinning type	General	1
F_{om} – Online monitoring	-	
F_{ip}- Adjustment for Injection/Mix Points	-	
F_{dl} - Adjustment for Dead-legs	-	

Table 8. *HIC/SOHIC-H₂S inspection results*

D_f $^{HIC\ SOHIC\ H2S}$ Hydrogen-induced Cracking and Stress-oriented Hydrogen-induced Cracking in Hydrogen Sulfide Services (HIC/SOHIC-H_2S) Inspection 1	
Date	1.01.1972
Damage mechanism	D_f $^{HIC\ SOHIC\ H2S}$
Effectiveness	Df HIC/SOHIC-H_2S - Inside - E: Ineffective
Sensitivity (Low, Medium, High)	Low
Water present (yes/no)	Yes
H_2S in water ppm	< 50 ppm
pH value	5.5 – 7.5
Cyanide (yes, no)	Yes
Steel product form (plate or pipe) and Sulfide content of plate steel	Product Form— Seamless/Extruded Pipe
Post weld heat treatment	Yes
F_{om} – Online monitoring	-

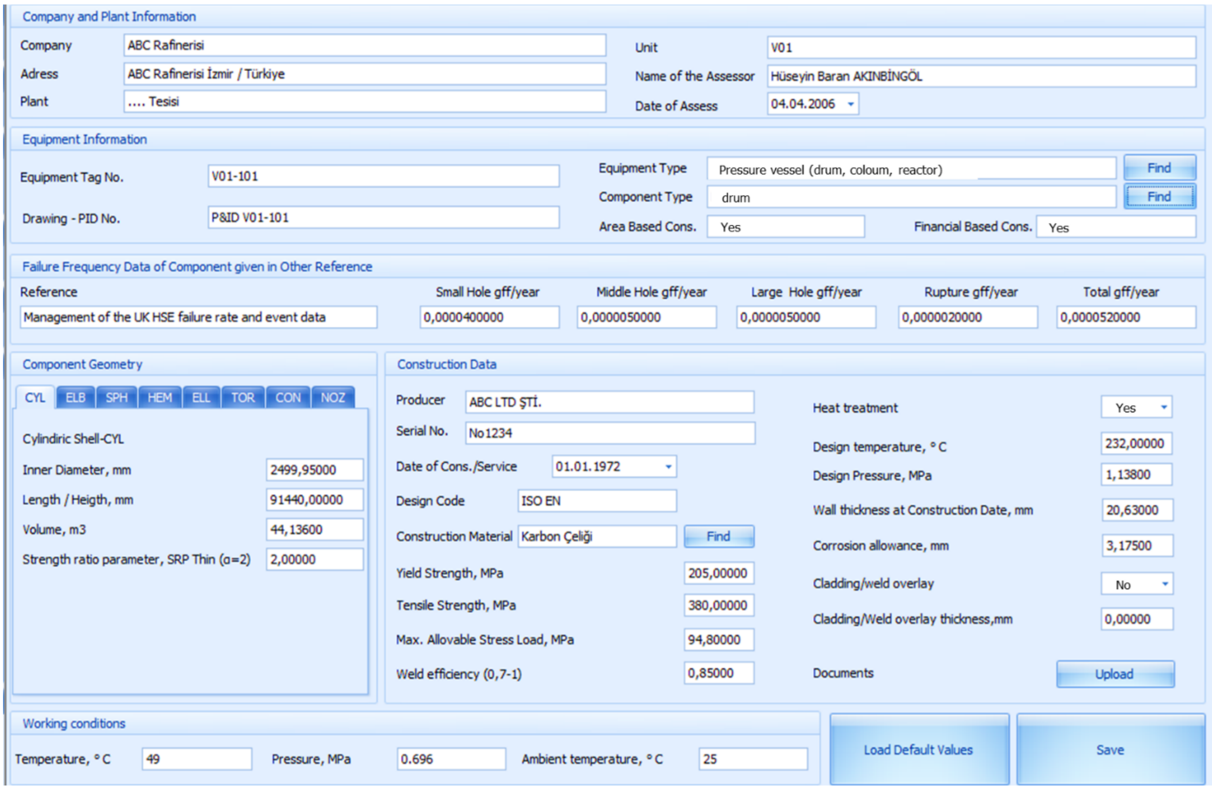

Figure 3. *Equipment and component data input to the software*

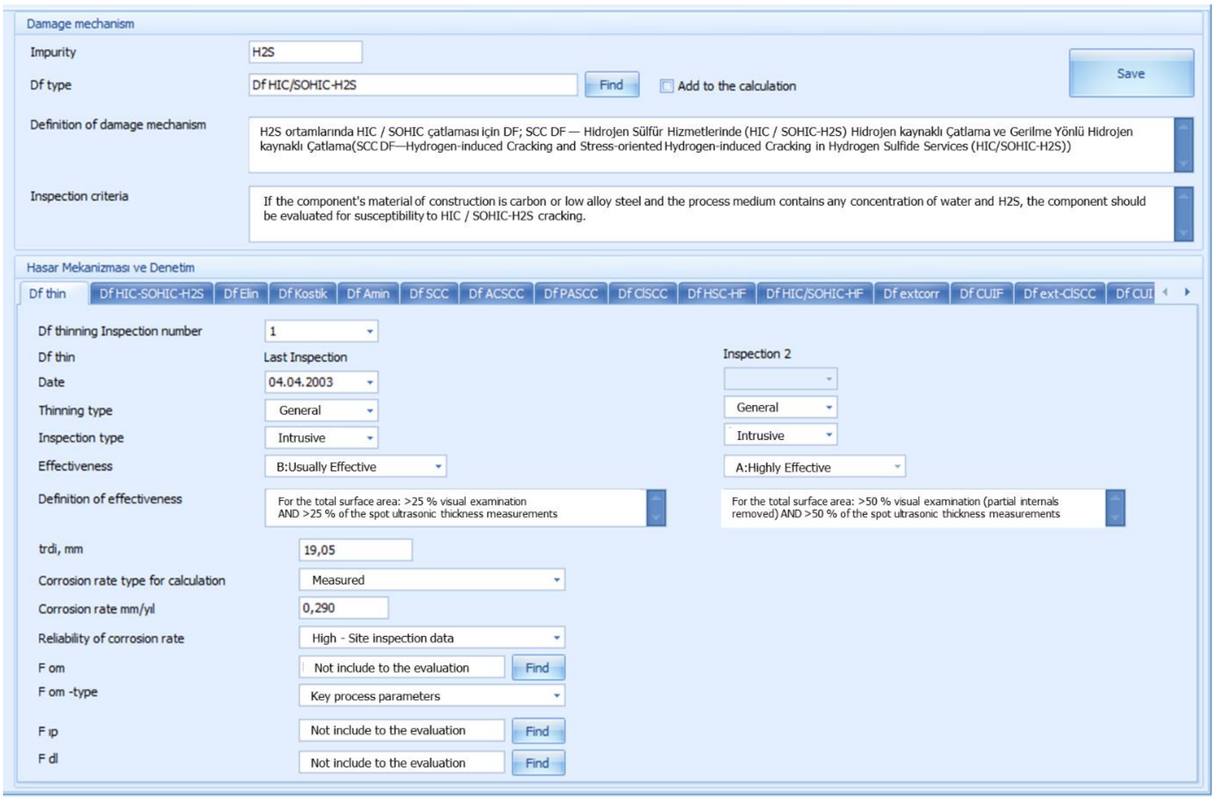

Figure 4. *Thinning corrosion mechanism data input to the software*

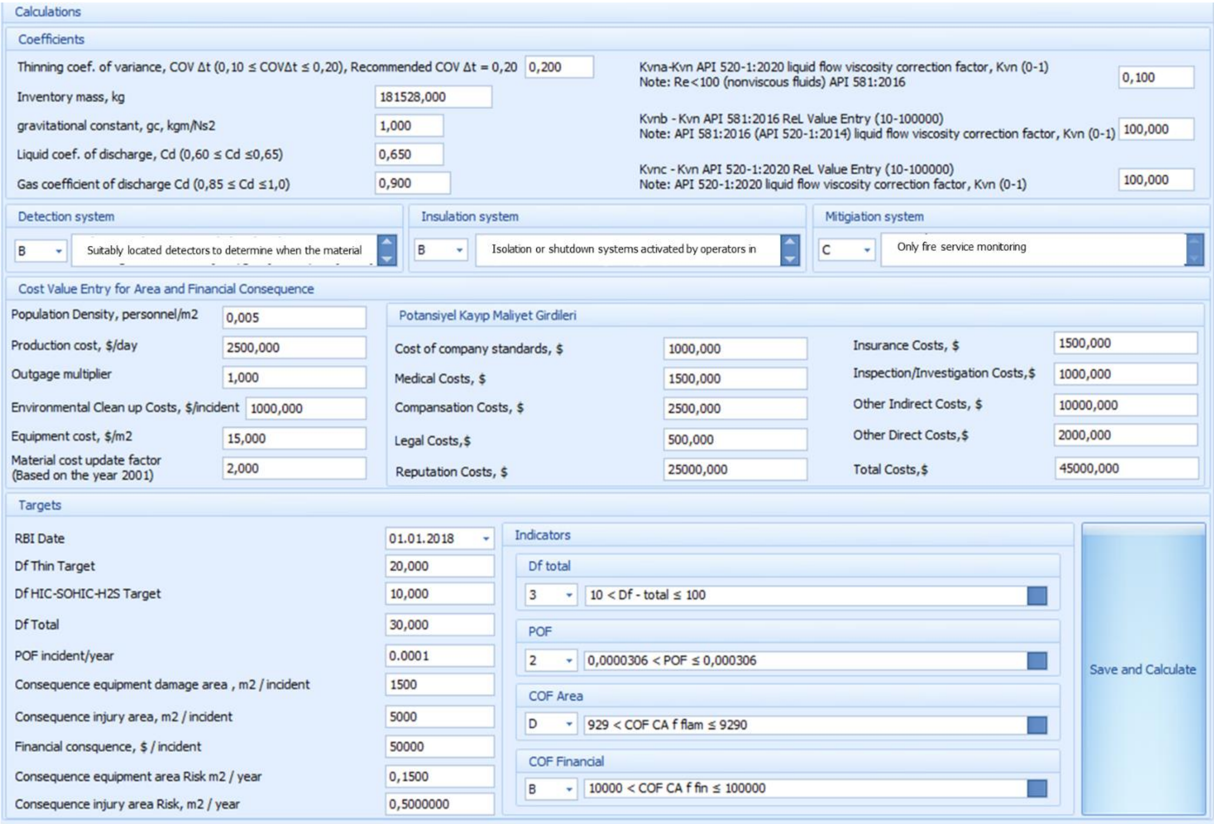

***Figure 5**. Result analysis data input to the software*

4. FINDINGS

As part of the case study, POF calculation was made for the date of 1.1.2018 over thinning and HIC/SOHIC-H_2S damage mechanisms. The GFF values taken from different references used in case study are shown at Table 9. The calculated POFs with equipment component generic failure frequencies taken from those references stated at Table 9 are given in Figure 6, and software screenshots are given in Figures 7 and 8.

***Table 9.** Probability of failure findings calculated with equipment component different GFF values*

Reference	Small Hole GFF	Medium Hole GFF	Large Hole GFF	Rupture GFF	Total GFF	POF
IOGP	2.6E-04	1.4E-05	3.8E-05	3.6E-05	3.8E-04	1.19E-02
Management of the UK HSE failure rate and event data	4.0E-05	5.0E-06	5.0E-06	2.0E-06	5.2E-05	1.78E-03
DNV leak	4.09E-04	2.23E-04	6.18E-05	5.93E-05	7.54E-04	2.58E-02
API RP 581	8.00E-06	2.00E-05	2.00E-06	6.00E-07	3.06E-05	1.048E-03

As that can be seen from Table 9, the GFF values used in case study are not same which are taken from different references. In the case study, those GFF values are used and calculated POF values based on the different GFF values are shown at the cells under POF at Table 9 and Figure 6. As the POF value increases GFF value also increases which is naturally expected as per the equation 1.

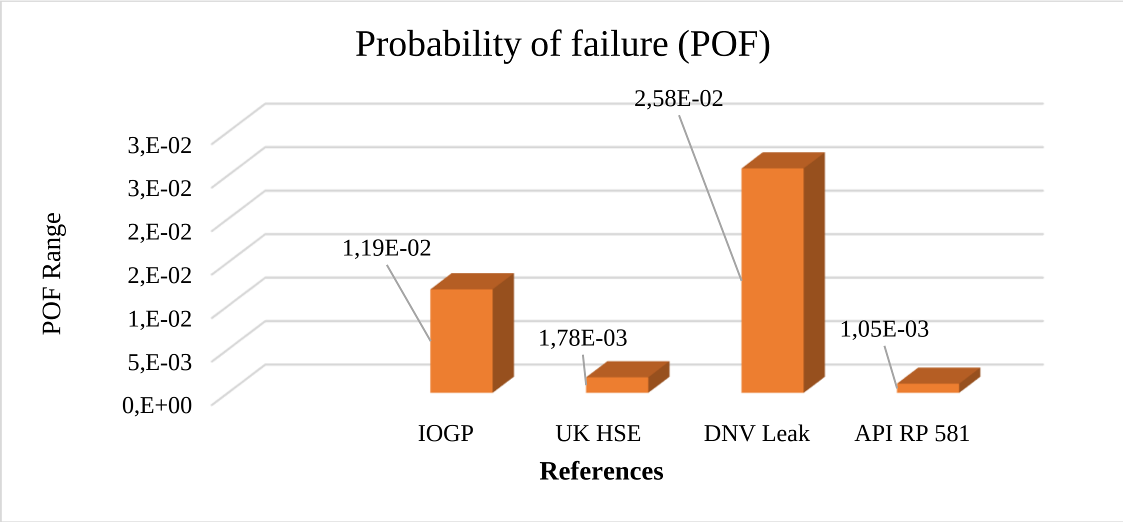

Figure 6. *Probability of failure findings calculated with equipment component different GFF values*

As that can be seen from Table 9, the GFF values used in case study are not same which are taken from different references. In the case study, those GFF values are used and calculated POF values based on the different GFF values are shown at Figure 6. The POF value increases as GFF value increases expected as per the equation 1.

The user interface for POF, COF and Risk calculation results are given at Figure 7 and 8. The POF results are given at Figure 7 based on GFF values taken from API RP 581 (see at Table 2 for drum and same as Table 9 for API RP 581). The POF results are given at Figure 8 based on GFF values taken from user input as from another reference (Keeley et al., 2011) (see Table 9 Management of the UK HSE failure rate and event data). The software also give POF, COF and risk results as matrix. At matrixes in Figure 7 and 8, the calculated risk category is found at orange area and in Figure 7 and found at yellow area in Figure 8. According to the results although the other values of variables are kept same for risk calculation except the GFF values, the different GFF values are effecting the calculated risk category which are important to decision making process for risk management.

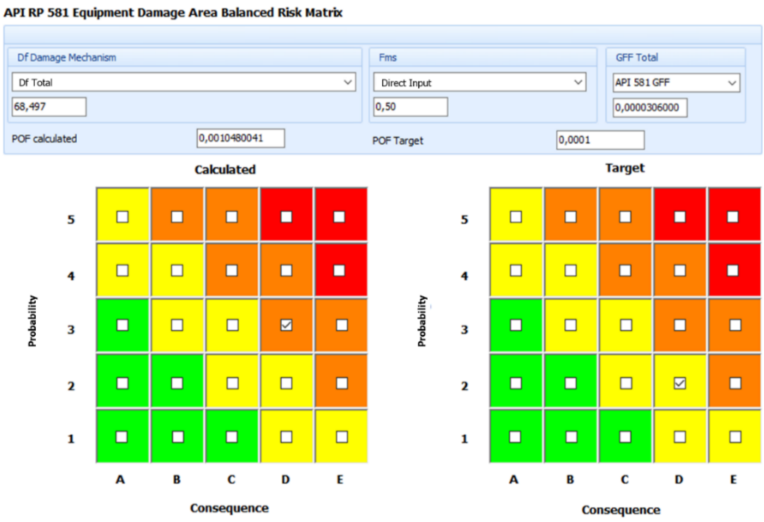

Numerical Values Associated with POF and Area-based COF Categories

Probability Category		Consequence Category	
Category	Probability Range	Category	Consequence Range
1	POF ≤ 0,0000306	A	COF CA f flam ≤ 9,29
2	0,0000306 < POF ≤ 0,000306	B	9,29 < COF CA f flam ≤ 92,9
3	0,000306 < POF ≤ 0,00306	C	92,9 < COF CA f flam ≤ 929
4	0,00306 < POF ≤ 0,0306	D	929 < COF CA f flam ≤ 9290
5	POF > 0,0306	E	COF CA f flam > 9290

Figure 7. *Screenshot of POF and other results calculated with API RP 581 GFF data*

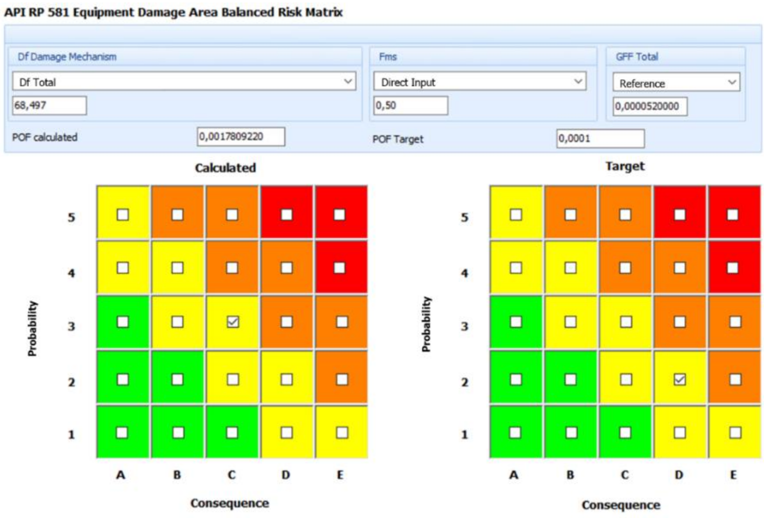

Numerical Values Associated with POF and Area-based COF Categories

Probability Category		Consequence Category	
Category	Probability Range	Category	Consequence Range
1	POF ≤ 0,0000306	A	COF CA f flam ≤ 9,29
2	0,0000306 < POF ≤ 0,000306	B	9,29 < COF CA f flam ≤ 92,9
3	0,000306 < POF ≤ 0,00306	C	92,9 < COF CA f flam ≤ 929
4	0,00306 < POF ≤ 0,0306	D	929 < COF CA f flam ≤ 9290
5	POF > 0,0306	E	COF CA f flam > 9290

Figure 8. *Screenshot of POF and other results calculated with GFF data from the sample reference*

5. CONCLUSION

API RP 581 sets out a detailed methodology for risk-based inspection as compared to other standards. For that reason, that's preferred for software developing. However, the data used for calculation within the methodology presented in API RP 581 are used directly in the software and different alternatives are not offered to the software users. In the literature, there are many studies on failure frequency data from different sources. In this study, it is focused on the POF value calculation results between the generic failure frequency data of the equipment component given in API RP 581 and the failure frequency values from other references are used. With a case study on the software developed in accordance with the methodology presented in API RP 581, findings on the POF values calculated when using different equipment component generic failure frequency data were obtained.

According to the findings, it was found that there was a difference of up to 1491% (14.91 times) between the POF value calculated based on the different generic failure frequency data used within the scope of the case study. Although the increase in the POF, increases the risk, requires more effective but more costly inspections, more effective detection, isolation and reduction systems in terms of result analysis, and increases in precautionary costs. This change in POF calculations, which can also be taken as the frequency of major industrial accidents, shows that the quality of the equipment component failure frequency data obtained from the experience in the industry is important.

Obtaining equipment component failure frequency data from industry from corrosion-induced integrity loss events and categorizing them according to not only the equipment component but also the corrosion damage mechanism type will increase the reliability of POF calculations. Software developed based on the methodology set forth in API RP 581 should be developed in a way that enables the use of equipment component generic failure frequency data, which can be obtained from different sources in the literature and in this study.

ACKNOWLEDGEMENT

This work supported by Computer Engineer Murat GÜLER.

CONFLICT OF INTEREST

No conflict of interest was declared by the authors.

REFERENCES

AIChE PERD, American Institute of Chemical Engineers (2020, August 27). (Accessed:20/12/2021) www.aiche.org/ccps/resources/process-equipment-reliability-database-perd

ASME PCC-3:2007 (2008). *Inspection Planning Using Risk-Based Methods*. American Society of Mechanical Engineers Standarts.

API RP 581:2016 (2016). *Risk-based Inspection Methodology* (3rd ed.). American Petroleum Institute (API) Standarts.

Baybutt, P. (2015). A critique of the Hazard and Operability (HAZOP) study. *Journal of Loss Prevention in the Process Industries*, 33, 52-58.

CCPS, Center for Chemical Process Safety (2014). *Guidelines for Initiating Events and Independent Protection Layers in Layer of Protection Analysis*. Wiley.

DNV-RP-G101 (2002). *Risk Based Inspection of Offshore Topsides Static Mechanical Equipment*. Det Norske Veritas Standarts.

DNV, Det Norske Veritas (2013), Failure Frequency Guidance: Process Equipment Leak Frequency Data for Use in QRA.

EN 16991 (2018). *Risk-based inspection framework*. European Standarts.

EEMUA 159 (2017). *Above ground flat bottomed storage tanks - a guide to inspection, maintenance and repair*. Engineering Equipment and Materials Users Association Publications.

EEMUA 206 (2006). *A Risk Based Inspection - a guide to effective use of the RBI process*. Engineering Equipment and Materials Users Association Publications.

IOGP, International Oil & Gas Producers (2019). (Accessed:14/01/2021) www.iogp.org/bookstore/product/risk-assessment-data-directory-process-release-frequencies

Keeley, D., Turner, S., & Harper, P. (2011). Management of the UK HSE failure rate and event data. *Journal of Loss Prevention in the Process Industries*, *24*(3), 237-241. doi:10.1016/j.jlp.2010.09.002

Pittiglio, P., Bragatto, P., & Site, C. D. (2014). Updated failure rates and risk management in process industries. *Energy Procedia*, *45*, 1364-1371. doi:10.1016/j.egypro.2014.01.143

CPR 18E (2005). Guidelines for quantitative risk assessment 'Purple Book'. Publication Series on Dangerous Substances (PSG3). Netherlands Ministry of Housing, Spatial Planning and the Environment.

Revie, R. W. (2015). *Oil and Gas Pipelines Integrity and Safety Handbook*. John Wiley & Sons, Inc.

Wood, M. H., Vetere Arellano, A. L., & Van Wijk, L. (2013). *Lessons learned from accidents in EU and OECD countries, Corrosion-Related Accidents in Petroleum Refineries*, The European Commission's science and knowledge service. doi:10.2788/37964

URL1, (2019, March 02). Regulation on prevention of major industrial accidents and lessening their adverse impacts *"Büyük Endüstriyel Kazaların Önlenmesi ve Etkilerinin Azaltılması Hakkında Yönetmelik"*. Official Gazette of the Republic of Turkey, No:30702. www.resmigazete.gov.tr/eskiler/2019/03/20190302-1.htm

Research Article / Araştırma Makalesi GU J Sci, Part A, 9(1): 25-32 (2022) https://doi.org/10.54287/gujsa.1082957

Gazi University
Journal of Science
PART A: ENGINEERING AND INNOVATION
http://dergipark.org.tr/gujsa

An Approach for Color Measurement of Irradiated Fresh Cilantro

Pelin YÜCEL[1*]

[1]*Turkish Energy, Nuclear and Mineral Research Agency, Ankara, Turkey*

Keywords
Cilantro
Irradiation
Image Analysis
Color Coordinates

Abstract

Food irradiation is widely accepted as a proven and effective postharvest treatment to reduce the bacterial contamination, extend the shelf life and maintain the food quality. Spices and herbs are the most commonly irradiated commercial products. Low dose irradiation causes no adverse effects on the visual quality of fresh herbs and spices. The appearance and color of food influence the consumer's product choice. Numerous studies are performed on the use of computer vision and image processing for the color evaluation in the food industry. In the present study, fresh cilantro was chosen as a model to estimate the change in the color parameters of gamma irradiated fresh cilantro leaves. Image analysis method was proposed as an alternative to conventional colorimeters for color measurement of irradiated fresh herbs and spices.

Cite

Yucel, P. (2022). An approach for color measurement of irradiated fresh cilantro. *GU J Sci, Part A*, *9*(1), 25-32.

Author ID (ORCID Number)

P. Yucel, 0000-0002-1581-8388

Article Process	
Submission Date	04.03.2022
Revision Date	11.03.2022
Accepted Date	24.03.2022
Published Date	28.03.2022

1. INTRODUCTION

Food irradiation is a technology applicable for all groups of foods, as functional properties, nutritional quality and sensory acceptability of foods are slightly affected. In a food system, there is an interaction between radiation and water and other biological systems, resulting in radiolytic products as oxidizing agents and changes are observed in the molecular structure of organic matter. Deoxyribonucleic Acid (DNA) is damaged by radiation, preventing reproduction of microorganisms, insects and gametes (Chauhan et al., 2009). Gamma rays of nucleides ^{60}Co and, to a lesser extent, ^{37}Cs or X-rays with energies up to 5 MeV, or accelerated electrons with energies up to 10 MeV are the sources of ionizing radiation for food processing. These sources are feasible for commercial use of irradiation as desired food preservative effects are achieved and no radioactivity is observed in foods or packaging materials (Farkas, 2004). Gray (Gy) is the international unit for the absorbed radiation dose; generally pasteurization doses are smaller than 10 kGy and sterilization doses are greater than 10 kGy. Irradiation is suitable for packaged products, as it causes minimum rise in the temperature of the product, hereby preventing recontamination or reinfestation of the product. Ionizing radiation treatment of foods is approved by World Health Organization, Food and Agricultural Organization, International Atomic Energy Agency and many countries for producing better and safer foods. Space foods for astronauts are sterilized by irradiation (Acheson & Steele, 2001).

Microbial decontamination of herbs and spices have been achieved by irradiation for more than 40 years. CODEX and most countries have allowed the use of irradiation (WHO, 1994; Chmielewski & Migdal, 2005). Doses greater than 10 kGy should not be applied to a food, except application of higher doses for technological purpose. In Turkey, radiation processing of food is controlled by Food Irradiation Legislation of Republic of Turkey Ministry of Agriculture and Forestry (URL1, 2019).

*Corresponding Author, e-mail: pelin.yucel@tenmak.gov.tr

Irradiation, compared with thermal treatment, leaves no chemical residues and is proven to be more effective against bacteria (Tjaberg et al., 1972; Loaharanu, 1994; Thayer et al., 1996; Olson, 1998; Sádecká, 2007). As heat sterilization of spices result in the loss of thermolabile aromatic volatiles and/or thermally induced changes, ionizing radiation is less harmful to the spices and can be applied in place of ethylene oxide and methyl bromide treatment. Minimal modifications on the quality attributes of food are observed.

The most suitable way for microbial safety of spices and herbs seemed to be gamma irradiation, resulting in no change in the quality (Lee et al., 2005). Extensive research is available on the application of irradiation for spices, herbs and vegetable seasonings. Andrews et al. (1995) observed a significant reduction at a dose of 5 kGy and total elimination of microbial contamination at 10 kGy, with no effect on flavor quality of dry ginger. Of nine aromatic herbs and spices irradiated at 10 kGy, quinone radical content of all samples increased while some samples showed significant decrease in total ascorbate and carotenoids content (Calucci et al., 2003).

Despite being well known decontamination method, less study has been performed for the treatment of fresh herbs. Electron beam irradiation can be applied for fresh herbs, like *Salvia Officinalis* and *Calendula Officinalis* (Minea et al., 2004). Electron beam treatment can be cost effective due to high throughput of e-beam processing (Khade et al., 2020). *Escherichia coli* O157:H7 inoculated on cilantro was effectively reduced by irradiation and chlorination while maintaining product quality (Foley et al., 2004). Low irradiation doses were shown to have a smaller effect on sensory quality of parsley leaves than drying and freezing. Irradiation doses up to 1.4 kGy extended the shelf-life of minimally processed parsley leaves to 30 days (Cătunescu et al., 2019). The visual quality of fresh mint was not affected by low irradiation doses and samples showed good quality for up to 9 days of storage (Hsu et al., 2010). A study of methanolic extracts of ten commercial herbs and spices irradiated in the range 0 - 30 kGy done by Polovka & Suhaj (2013) showed that the observed changes in antioxidant activity induced by γ-irradiation were without practical significance and would have no negative effect on the health of the consumer.

Consumer's choice and preferences are generally influenced by color. Visual, instrumental and machine vision systems are applied for color measurement of many food products, including fruits and vegetables, spices and flavors, cereals and grains. Compared to the colorimetry and spectrophotometry, machine vision with digital imaging has advantages, namely analysis of the whole sample surface and objective evaluation of irregular color or surface (Giese, 2003). Machine vision with image processing has been found increasingly useful in the food industry. Brosnan & Sun (2004) reviewed the application of computer vision system and image processing in the food industry, mainly fruits and vegetables, meat, fish, pizza, cheese, bread and grain. There is an increasing trend in the use of machine vision system for the measurement of color. Machine vision system has the following parts; a camera linked to a computer, controlled lighting and software for camera settings, image capture and image processing. The image can be evaluated immediately or stored for further analysis (Balaban & Odabasi, 2006). Minz & Saini (2021) suggested computer vision system to measure the color of mozzarella cheese as an option to spectrophotometer. Although color spectrophotometer limits the measuring area, computer vision system permits the user to measure the color over the whole surface. Computer vision system is recommended as a rapid and low-cost quantification instrument.

Generally, fresh herbs, such as fresh cilantro, parsley and basil, are eaten raw and widely used as seasoning in many meals without any treatment step for microbial treatment. Herbs, which are grown low to the ground, can be contaminated easily from irrigation water (US FDA, 2022). Cilantro (*Coriandrum sativum*) is annual and herbaceous plant from the Apiceae family, originating from Mediterranean region. The leaves and stems are used to flavor dishes. The mature seeds are called coriander and used for flavoring (Abascal & Yarnell, 2012). Cilantro is a herb consumed worldwide and shows a wide range of health benefits from antibacterial to anticancer effects (Mauer & El-Sohemy, 2012). Khade et al. (2020) studied the effect of combined treatment of washing with potable water, sodium hypochlorite and radiation at 2 kGy to ensure safety and to eliminate the microbial load of coriander, mint and spinach. Shelf life was extended up to 15 days at 4-6°C by the developed combination. Irradiation of spices and herbs has a high potential application in many countries. The objective of this study was to determine a relationship between color parameters of fresh cilantro leaves subjected to irradiation with a simple computer vision system. The color of irradiated fresh cilantro was compared with non-irradiated cilantro.

2. MATERIALS AND METHODS

Fresh cilantro samples were supplied by commercial grade and placed in polyethylene bags. 0, 1, 2 and 3 kGy (at a dose rate of 0,626 kGy/h from a Cobalt-60 source) irradiation doses were applied at Turkish Energy, Nuclear and Mineral Research Agency, Ankara, Turkey. Non- irradiated samples were used as controls. The absorbed doses were controlled by alanine dosimetry.

The measurements were made with a simple computer vision system (CVS). Image analysis is the core of this system. The objects are distinguished from the background and quantitative information is produced to be used in the control systems (Brosnan & Sun, 2004). Images of samples were captured by a scanner in jpeg format with a resolution of 300 dpi and a region of interest (ROI) was selected to obtain color information (Figure 1). Intensity values of ROI were read from the image for each color coordinate system (CIE XYZ, CIE L*a*b*, Hunter Lab and RGB). The programme BAB BS200ProP was used to process the color parameters. BAB BS200ProP image analysis system enables the user to acquire images from external sources, such as camera, scanner and keep the images in a database.

Figure 1. *Color measurement from image of scanned cilantro leaves*

Of the color parameters, the ratio of white to black, red to green, and yellow to blue are represented by L* value, a* value and b* value, respectively. Positive values of a* indicate red color and negative values indicate green color. Positive values of b* are measured for yellow color and negative values are for blue color. Color saturation or intensity is measured by chroma. Hue angle (h°) defines the comparative amount of redness and yellowness, where angle of 0°/360°, 90°,180° and 270° indicates red/magenta, yellow, green and blue color or purple or intermediate color between neighboring pair of basic colors (McGuire,1992). Hue angle and chroma were calculated from a* and b* color space, done by using the formulae (Wrolstad & Smith, 2010).

$$hue\ angle\ (°) = \arctan\left(\frac{b^*}{a^*}\right) \quad (1)$$

$$chroma = \sqrt{(a*^2 + b*^2)} \quad (2)$$

3. RESULTS AND DISCUSSION

Color is an important quality index and plays a main role for consumer preferences and consumer acceptability. *RGB* (red, green, blue), Hunter Lab, *CIE* (Commission Internationale de l'Eclairage) *L*a*b**, *CIE XYZ, CIE Yxy* and *CIE LCH* are the color coordinate systems used to define color a sample (Giese, 2003). Of the color spaces, most commonly used system in the food industry is *CIE L*a*b**, owing to its uniform color distribution, as well as the perception system is very near to the human eye (Markovic et al., 2013). In this study, color changes observed after irradiation were evaluated by image analysis system in *L*a*b** model system of fresh cilantro (Table 1).

Table 1. *Color parameters of non-irradiated and irradiated fresh cilantro*

Dose (kGy)	RGB			CIE L*a*b*			Hunter Lab		
0	111	155	79	59.33	-28.86	34.9	52.33	-24.4	23.4
1	105	147	73	56.44	-27.99	34.4	49.35	-23.1	22.4
2	102	144	71	55.3	-27.92	34.0	48.19	-22.8	21.9
3	99	141	70	54.18	-27.72	33.1	47.06	-22.5	21.3

L* value, which is the color coordinate characterizing the lightness, decreased upon irradiation (Figure 2a). During irradiation, L* values showed a decrease in all treatments, being higher in control compared to irradiated samples (Table 1). The observed values were of the range 59.33-54.18. No significant effect was observed on aroma, amount of total volatile compounds, color or overall visual quality of fresh cilantro leaves irradiated at doses up to 2 kGy (Fan et al., 2003). L* value decreased as radiation dose increased in dry smoked shrimp. Increasing radiation dose resulted in a trend of decrease in whiteness (Akuamoah et al., 2018). Significant decrease was monitored in the appearance, color and texture of fresh spinach after irradiation (Al-Suhaibani & Al-Kuraieef, 2016). Undesirable changes in the sensory quality of foods can be prevented by the selection of suitable dose. Irradiation of fresh-cut iceberg lettuce and spinach at doses of 1 and 2 kGy enhanced the microbial safety while maintaning quality (Fan et al., 2012).

Chroma value, proportional to the strength of the color, shows the degree of saturation of color. A change was observed in the chroma between the non-irradiated and irradiated samples. The highest chroma value was observed for non-irradiated sample (Figure 2b). The observed chroma values were of the range 45.29-43.17. A general trend of decrease was noted in chroma values (Table 2). Control quince fruits, either due to browning or chlorophyll degradation, showed higher chroma values compared to irradiated fruits (Hussain et al., 2019). When gamma irradiation and low energy electron beam treatment were compared for allspice berries, caraway seeds, oregano and rosemary leaves, no difference was found in color, water activity, chlorophyll and caretonoid contents and terpenoic compounds for storage time up to 105 days (Schottroff et al., 2021). Irradiation would have no adverse effect on the acceptability of fresh herbs.

The hue angle (h°), where values above 100°C representing green color and values below 90°C yellow color, is often used for color determination. In our study, the highest value was obserbed for 3 kGy irradiation. (Figure 2c). The hue angle range was within the 120° region, suggesting green color. The observed hue angle values were of the range 129.13-129.95. The lower the irradiation dose employed the less undesired effects were observed for products containing organic colors (Reid, 1995). For fresh mushrooms and dried mushrooms, good linear correlations were reported by Kortei et al. (2015) between the hue angle and the lightness after irradiation. Irradiation had no adverse effect on product quality. Knowledge of the effect of irradiation on the color of the food products can be used to decide the optimum irradiation dose for the food.

a)

b)

c)

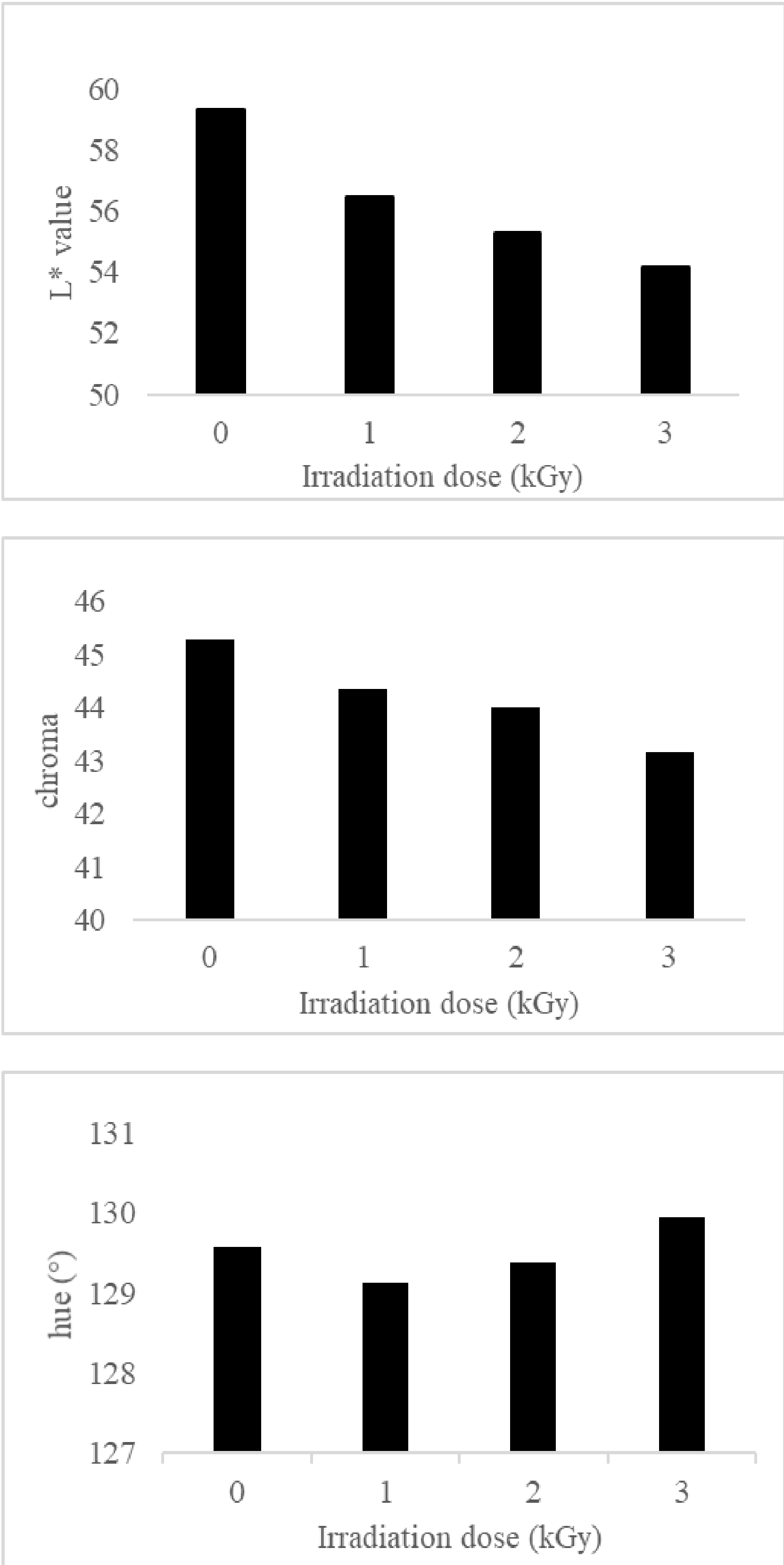

Figure 2. a) *Color lightness,* ***b)*** *chroma and* ***c)*** *hue angle,*
for non-irradiated and irradiated fresh cilantro

Table 2. *Chroma and hue angle values of non-irradiated and irradiated fresh cilantro*

Dose (kGy)	L* value	chroma	hue (º)
0	59.33	45.29	129.59
1	56.44	44.35	129.13
2	55.30	43.99	129.39
3	54.18	43.17	129.95

4. CONCLUSION

Food quality and safety are important for the food industry. Food irradiation is a suitable technology for fresh herbs and spices, as ionizing radiation effectively inhibits physical changes during postharvest deterioration and maintains a fresh product appearance. Instrumental color measurement combined with image processing eliminates the limitations of the subjective human sensory analysis In this study, computer vision system with image processing is utilized to measure the color of irradiated fresh cilantro. The study has been conducted on the images of fresh cilantro which are captured before and after irradiation. This study proposes that color can be measured only by using a simple scanner, avoiding the use of an expensive colorimeter. Tristimulus values can be converted into other color systems. The color lightness (L*) decreased when fresh cilantro was irradiated. A change in chroma value was observed between the fresh and irradiated cilantro; fresh cilantro showing the highest chroma value (45.29). The hue angle (h°) was highest at 2 kGy. Image analysis can be a viable technique to measure the color of irradiated foods, providing better characterization of irradiated foods and improving irradiated food quality.

ACKNOWLEDGEMENT

Author would like to thank to the Turkish Energy, Nuclear and Mineral Research Agency.

CONFLICT OF INTEREST

No conflict of interest was declared by the author.

REFERENCES

Abascal, K., & Yarnell, E. (2012). Cilantro-Culinary Herb or Miracle Medicinal Plant?. *Alternative and Complementary Therapies*, *18*(5), 259-264. doi:10.1089/act.2012.18507

Acheson, D., & Steele, J. H. (2001). Food Irradiation: A Public Health Challenge for the 21st Century. *Clinical Infectious Diseases*, *33*(3), 376-377. doi:10.1086/321899

Akuamoah, F., Odamtten, G. T., & Kortei, N. K. (2018). Influence of gamma irradiation on the colour parameters of dry smoked shrimps (*Penaeus notialis*). *Food Research*, *2*(4), 350-355. doi:10.26656/fr.2017.2(4).0271

Al-Suhaibani, A. M., & Al-Kuraieef, A. N. (2016). The Effects of Gamma Irradiation on the Microbiological Quality, Sensory Evaluation and Antioxidant Activity of Spinach. *International Journal of Chem Tech Research*, *9*(6), 39-47.

Andrews, L. S., Cadwallader, K. R., Gronder, R. M., & Chung, H. Y. (1995). Chemical and microbial quality of irradiated ground ginger. *J. Food Sci.*, *60*(4), 829-832. doi:10.1111/j.1365-2621.1995.tb06240.x

Balaban, M. O., & Odabasi, A. Z. (2006). Measuring color with machine vision. *Food Technology*, *60*(12), 32-36. (makalenin son haline eklenmeyecek – makale yılını kontrol etmek için bağlantı adresi)

Brosnan, T., & Sun, D-W. (2004). Improving quality inspection of food productsby computer vision—a review. *Journal of Food Engineering*, *61*(1), 3-16. doi:10.1016/S0260-8774(03)00183-3

Calucci, L., Pinzino, C., Zandomeneghi, M., Capocchi, A., Ghiringhelli, S., Saviozzi, F., Tozzi, S., & Galleschi, L. (2003) Effects of gamma-irradiation on the free radical and antioxidant contents in nine aromatic herbs and spices. *J Agric Food Chem*., *51*(4), 927-34. doi:10.1021/jf020739n

Cătunescu, G. M., Muntean, M., Marian, O., David, A. P. & Rotar, A. M. (2019). Comparative effect of gamma irradiation, drying and freezing on sensory and hygienic quality of parsley leaves. *Lebensmittel-Wissenschaft und-Technologie, 115*, 108448. doi:10.1016/j.lwt.2019.108448

Chauhan, S. K., Kumar, R., Nadanasabapathy, S., & Bawa, A. S. (2009). Detection Methods for Irradiated Foods. *Comprehensive Reviews in Food Science and Food Safety*, *8*(1):4-16. doi:10.1111/j.1541-4337.2008.00063.x

Chmielewski, A. G. & Migdal, W. (2005). Radiation decontamination of herbs and spices. *Nukleonika*, *50*(4): 179-184.

Fan, X., Niemira, B. A., & Sokorai, K. J. B. (2003). Sensorial, nutritional and microbiological quality of fresh Cilantro leaves as influenced by ionizing radiation and storage. *Food Research International*, *36*(7), 713-719. doi:10.1016/S0963-9969(03)00051-6

Fan, X., Guan, W., & Sokorai, K. J. B. (2012). Quality of fresh-cut iceberg lettuce and spinach irradiated at doses up to 4 kGy. *Radiation Physics and Chemistry*, *81*(8), 1071-1075. doi:10.1016/j.radphyschem.2011.11.022

Farkas, J. (2004) Food Irradiation. In: A. Mozumder, Y. Hatano (Eds.), *Charged particle and photon interactions with matter* (pp. 785-812). Marcel Dekker Inc., New York-Basel.

Foley, D., Euper, M., Caporaso, F., & Prakash, A. (2004). Irradiation and chlorination effectively reduces *Escherichia coli* O157:H7 inoculated on cilantro (*Coriandrum sativum*) without negatively affecting quality. *J. Food Prot.*, *67*(10), 2092-2098. doi:10.4315/0362-028X-67.10.2092

Giese, J. (2003). Color Measurement in Foods. *Food Technology*, *57*(12), 48-49+54.

Hsu, W-Y., Simonne, A., Jitareerat, P., & Marshall Jr., M. R. (2010). Low-dose irradiation improves microbial quality and shelf life of fresh mint (Mentha piperita L.) without compromising viual quality. *J. Food Sci.*, *75*(4), M222-M230. doi:10.1111/j.1750-3841.2010.01568.x

Hussain, P. R., Rather, S. A., Suradkar, P. P., & Ayob, O. (2019). Gamma irradiation treatment of quince fruit (*Cydonia oblonga* Mill): effect on post-harvest retention of storage quality and inhibition of fungal decay. *Journal of Radiation Research and Applied Sciences*, *12*(1), 118-131.

Khade, H. D., Hajare, S. N., Sarma, K. S. S., & Gautam, S. (2020). A combination process including ionizing radiation for hygienization and shelf life extension of leafy vegetables. *Indian Journal of Experimental Biology*, *58*, 474-486.

Kortei, N. K., Odamtten, G. T., Obodai, M., Appiah, V., & Akonor, P. T. (2015). Determination of color parameters of gamma irradiated fresh and dried mushrooms during storage. *Croatian Journal of Food Technology*, *Biotechnology and Nutrition*, *10*(1-2), 66-71.

Lee, J. H., Lee, K-T., & Kim, M. R. (2005). Effect of Gamma-Irradiated Red Pepper Powder on the Chemical and Volatile Characteristics of Kakdugi, a Korean Traditional Fermented Radish Kimchi. *Journal of Food Science*, *70*(7), 441-447. doi:10.1111/j.1365-2621.2005.tb11466.x

Loaharanu, P. (1994). Status and prospects of food irradiation. *Food Technology*, *52*, 124-131.

Markovic, I., Ilic, J., Markovic. D., Simonovic, V., & Kosanic, N. (2013) Color Measurement of Food Products Using CIE L*a*b* and RGB Color Space. *Journal of Hygienic Engineering and Design*, *4*, 50-53.

Mauer, L., & El-Sohemy, A. (2012). Prevalence of cilantro (Coriandrum sativum) disliking among different ethnocultural groups. *Flavour*, *1*, 8. doi:10.1186/2044-7248-1-8

McGuire, R. G. (1992). Reporting of objective color measurements. *HortScience*, *27*(12), 1254-1255. doi:10.21273/HORTSCI.27.12.1254

Minea, R., Nemtanu, M. R., Brasoveanu, M., Oproiu, C., Mazilu, E., & Radulescu, N. (2004). *Accelerators use for irradiation of fresh medicinal herbs*. In: Proceedings of EPAC 2004, Switzerland, (pp. 2368-2370).

Minz, P. S., & Saini, C. S. (2021). Comparison of computer vision system and colour pectrophotometer for colour measurement of mozzarella cheese. *Applied Food Research*, *1*(2). doi:10.1016/j.afres.2021.100020

Olson, D. G. (1998). Irradiation of food. *Food Technology*, *52*, 56-62.

Polovka, M, & Suhaj, M. (2013). Classification and prediction of γ-irradiation of ten commercial herbs and spices by multivariate evaluation of properties of their extracts. *Journal of Food and Nutrition Research*, *52*(1), 45-60.

Reid, B. D. (1995). Gamma processing technology: an alternative technology for terminal sterilization of parenterals. *Journal of Pharmaceutical Science and Technology*, *49*(2), 83-89.

Sádecká, J. (2007). Irradiation of Spices- a Review. *Czech J. Food Sci.*, *25*(5), 231-242.

Schottroff, F., Lasarus, T., Stupak, M., Hajslova, J., Fauster, T., & Jäger, H. (2021). Decontamination of herbs and spices by gamma irradiation and low-energy electron beam treatments and influence on product characteristics upon storage. *Journal of Radiation Research and Applied Sciences*, *14*(1), 380-395.

Thayer, D. W., Josephson, E. S., Brynjolfsson A., & Giddings G.G. (1996). Radiation Pasteurization of Food. *Council for Agricultural Science and Technology*, *7*, 1-10.

Tjaberg, T. B., Underdal, B., & Lunde, G. (1972). The effect of ionizing radiation on the microbial content and volatile constituents of spices. *Journal of Applied Bacteriology*, *35*(3), 473-478. doi:10.1111/j.1365-2672.1972.tb03724.x

URL1, (2019, October 03). Food Irradiation Legislation *"Gıda Işınlama Yönetmeliği"*. Official Gazette of the Republic of Turkey, No:30907. www.resmigazete.gov.tr/eskiler/2019/10/20191003-1.htm

US FDA, US Food and Drug Administration (2022, March 14). Microbiological Surveillance Sampling: FY18-21 Fresh Herbs (Cilantro, Basil & Parsley) Assignment. www.fda.gov/food/sampling-protect-food-supply/microbiological-surveillance-sampling-fy18-21-fresh-herbs-cilantro-basil-parsley-assignment

WHO, World Health Organization (1994). Safety and nutritional adequacy of irradiated food. World Health Organization, Geneva. https://apps.who.int/iris/handle/10665/39463.

Wrolstad, R. E., & Smith, D. E. (2010) Colour Analysis. In: S. S. Nielsen (Eds.), *Food Analysis* (pp. 545-555). Springer Science+Media, New York, USA.

Research Article / Araştırma Makalesi GU J Sci, Part A, 9(1): 33-40 (2022) https://doi.org/10.54287/gujsa.1084430

Gazi University
Journal of Science
PART A: ENGINEERING AND INNOVATION
http://dergipark.org.tr/gujsa

Relationship Between Hydrocarbon Content and Oxidative Stability in Irradiated Hazelnut Oils

Hülya GÜÇLÜ[1*]

[1]*Turkish Energy, Nuclear and Mineral Research Agency, Ankara, Turkey*

Keywords

Gamma Irradiation

Hydrocarbon(s)

Rancimat

Induction Time

Hazelnut Oil

Abstract

The hydrocarbon detection method, based on the detection of hydrocarbons formed during irradiation, is one of the internationally accepted detection methods for irradiated foods. Radiolysis products, formed due to breakdown of unsaturated fatty acids by irradiation, are detected in this method. While no hydrocarbons were not found in the unirradiated hazelnut oil, hydrocarbons, namely 1-7 hexa-decadiene, 1- hexa-decene, n-penta-decane and 1- tetra-decene, but they were detected after irradiation at doses of 5 kGy or higher. It was found that irradiation induced the formation of hydrocarbons and when irradiation dose increased, the amount of hydrocarbons increased. The Rancimat process is widely used to define the amount of oxidation in foods containing fat. Analysis time is short as it is a very fast method. The induction time, showing the oxidation resistance of oils, decreased as irradiation dose increased. The possible relationship between the detected hydrocarbons and oxidative stability was examined and a negative correlation was found between the hydrocarbon and rancimat methods.

Cite

Guclu, H. (2022). Relationship between hydrocarbon cntent and oxidative stability in irradiated hazelnut oils. *GU J Sci, Part A, 9*(1), 33-40.

Author ID (ORCID Number)

H. Güçlü, 0000-0003-1610-8051

Article Process

Submission Date	08.03.2022
Revision Date	16.03.2022
Accepted Date	24.03.2022
Published Date	28.03.2022

1. INTRODUCTION

Food irradiation is a technology applicable for all groups of foods, as nutritional, functional and sensory properties of food products are slightly affected. In a food system, there is an interaction between radiation and water and other biological systems, resulting in radiolytic products, acting as oxidizing agents and changes in the molecular structure of organic matter are observed. Deoksi-ribonükleik asit molecules are damaged by radiation and inhibit the reproduction of microorganisms, insects and gametes. Chauhan et al. (2009).

High-energy-photons sourses (Gamma rays with 60-Co and 37-Cs nuclei), X-rays is produced by machines with energies of 5 MeV and electron accelerator machines are used in food irradiation process. These sources are feasible for commercial use of irradiation as desired food preservative effects are achieved and no radioactivity is observed in foods or packaging materials Farkas (2004). Gray (Gy) is the international unit for the absorbed radiation dose; generally pasteurization doses are <10 kGy are and sterilization doses are >10 kGy. It can perform irradiation on packaged products, as it creates minimal temperature rise in the product and can be used through packaging materials, hereby preventing recontamination or reinfestation of the product.

The World-Health Organization, the Food and Agricultural Organization, the International- Atomic-Energy-Agency and many countries confirm food irradiation for producing better and safer foods. Space foods for astronauts are sterilized by irradiation (Acheson & Steele, 2001).

*Corresponding Author, e-mail: hulya.guclu@tenmak.gov.tr

Microbial decontamination of herbs and spices have been assured by irradiation for more than 40 years. CODEX and most countries have allowed the use of irradiation (WHO, 1994; Chmielewski & Migdal, 2005). Doses greater than 10 kGy should be used to a food, except for application of higher doses for technological doses. In Turkey, radiation processing of food is controlled by Food Irradiation Legislation of Republic of Turkey Ministry of Agriculture and Forestry (URL1, 2019).

In previous studies, irradiation was more effective than heat treatment against bacteria, while leaving no chemical residues (Tjaberg et al., 1972; Loaharanu, 1994; Thayer et al., 1996). While heat sterilization of spices causes the loss of causes thermally induced changes, thermolabile aromatic volatiles or, such as decomposition brought about by high temperatures or production of thermally induced radicals, food irradiation is less harmful to the spices and can be applied in place of ethylene oxide and methyl bromide treatment. Minimal modifications on the quality attributes of food are observed (Olson, 1998; Sádecká, 2007).

Hazelnut production in Turkey is very high due to the favorable weather conditions. Turkey is one of the main producer, as well as the largest hazelnut exporter in the world. Turkey accounts for 75% of the world hazelnut production and approximately 70-75% of this production is exported to more than 90 countries in the world (URL2, 2012).

Hazelnuts are commercially irradiated in the range of 1-5 kGy to control insects, reduce the number of microorganisms and extending the shelf life of food (URL3, 1999). Although appropriate labeling of irradiated foods is mandatory, there is the possibility that they have been irradiated without any notification on the shipment (EN 1784, 2003).

To prevent this, there are ten current methods used to identify the irradiated foods. The European Standard EN 1784:2003 is used for the determination of hydrocarbons formed as a result of irradiation of oil-containing foods. It is a method based on gas chromatographic detection of hydrocarbons formed by radiation (Kader, 1986). When food is irradiated, different hydrocarbons are formed by the breakdown of fatty acids, some of them are found excessively, one with one fewer carbon than the main-fatty acid (n-1), and the other with two fewer carbons with an extra doubl-bond at position 1 (n-2, 1-ene) (Spiegelberg et al., 1994).

Hazelnut oil, its high content (more than 40%), is widely consumed in diet. Since the level of unsaturated fatty acids is high in hazelnut oils, irradiation causes oxidation of these fatty acids. These poly-unsaturated fatty acids are attacked by oxygen to yield peroxides, which then further decompose (Mexis et al., 2009). Oxidative stability is the main factor for determining the shelf life of high fat containing foods, such as hazelnuts. The Rancimat method is one of the most widely used methods, as it can detect oxidation easily and quickly in a very short time (Mendez et al., 1996). The oxidative stability depends on the acyl-glycerol composition and on the amount and type of minor components in oil (Mateos et al., 2005). In addition, this method does not require periodic work and chemicals (Hasenhuettl & Wan, 1992).

The aim of our study was to detect the formation of hydrocarbons in gamma irradiated hazelnut oils by gas chromatography (GC). Meanwhile, the Rancimat Method was used to determine the oxidative stability of the samples. The existence of possible correlation between the hydrocarbon method and Rancimat method was evaluated to examine the effect of irradiation in hazelnut oils.

2. MATERIALS AND METHODS

2.1. Samples

Hazelnut samples (Corylus avellana L.-Ordu variety, unshelled) used in this study were obtained from a regional market in Ankara, Turkey. Hazelnut samples were individually weighed into polyethylene bags for irradiation. Polyethylene bags were used because they are light, irresponsive to biological agents, robust to chemical substances and atmospheric conditions, unaffected by temperature changes between 60 and 200°C. All samples were stored in the refrigerator (± 4°C) until and after irradiation.

Lipid extraction

Finely chopped hazelnuts (10 g) were extracted by shaking the seeds with 30 mL of hexane/isopropanol (3:2, v/v) for 1 hour in steel tubesThe solutions were filtered under vacuum and the residues washed twice with 20 mL of the same solvent. 35 mL of sodium sulfate (6.72%) was added and the top layer was evaporated under vacuum at 40°C. The oils were stored at 4°C (Thayer et al., 1996).

2.2. GC Analysis of Hydrocarbons

Analysis of hydrocarbons in the samples, obtained by extraction of irradiated hazelnut oils, was performed using gas chromatograph (6980 series Hewlett-Packard Co. Wilmington, DE). The gas chromatography detector used in the analysis was a flame ionization detector (FID) with splitless injection. Carrier gas was helium, flow rate was set to 2.6 mL/min. The column in the analysis was a DB-5[(phenyl-5%)-methyl-polysiloxane] of 0.25mm i.d.x30m with a 0.25 µm film thickness. The column temperature was initially set at 50°C for 2 minutes and programmed at 10°C/min to 70°C, 2.5°C/min to 170°C, and 10°C/min to 280°C and 5 minute final hold. The detector and injector temperatures were respectively 250°C and 200°C. Samples (1 µL) diluted with hexane were injected into the instrument.

All experiments were repeated three times. Identification of hydrocarbon peaks was based on retention time as compared to hydrocarbon standards of 1-tetradecene, n-pentadecane and 1,7-hexadecadiene (Fluka Analytical), and 8-hexadecen (Sigma-Aldrich Corporation). The results were calculated by using the standard curves obtained for each of four hydrocarbons (Choi & Hwang, 1997).

2.3. Measurement of Oxidative Stability

Rancimat (Metrohm apparatus model 743, Switzerland, Herisau) was used to measure the oxidation level of oils in irradiated hazelnut samples. The operating temperature range of this device is 50-200°C. The processing temperature is set to 120°C. The airflow rate was set at 20 L/h for all analyses. Each oil sample was weighed 3.5±0.1g into the reaction vessel and placed on the heating block. It was filled with 60 mL of distilled water. The volatile compounds resulting from the breakdown of oils were gathered in a receiving flask during measurement.

The conductivity and the induction times were measured automatically by apparatus software. Induction time was taken as the time that corresponded to the point of sharp increase in conductivity, where the baseline tangent to the conductivity curve starts, and expressed in hours (Frank et al., 1982). All analyses were repeated in duplicate**.**

RESULTS AND DISCUSSION

As with other oil seeds, hazelnut oil contains mono-unsaturated fatty acids, oleic acid. İt is usually found the highest. This is followed by ***linoleic acid***, which is a binary unsaturated fatty acid (Choi & Hwang, 1997). For this reason, oxidative deterioration occurs easily in hazelnut oils. The presence of hydrocarbons in oil-containing foods is the most important indicator of the irradiation process applied to the food.

In our studies, no hydrocarbons were detected in the oil extracted from the naturel hazelnuts (Table 1). As shown in the Table 1, ***1-7 hexadecadiene*** reached a very high value (10.42 ppm) in hazelnut oil irradiated at 5 kGy. ***n-pentadecane*** and ***1-tetradecene***, possibly from palmitic acid, were not found in unirradiated hazelnuts but were found in hazelnuts irradiated at 0.5 kGy or higher. When oil irradiated 5 kGy doses they reach the value of 1.02 and 0.89 ppm, respectively. ***1-hexadecene***, was found at fairly high levels in the samples irradiated at 0.5 kGy or higher. The value of the analysis results are given in Figure 1.

In parallel with the increase in the irradiation dose, a linear increase occurred especially in the amount of *1-tetradecene* (R^2=0.990) and *n-pentadecane* (R^2=0,982). The highest increase in the amount of hydrocarbons in the irradiated oils was determined at 5 kGy dose. As seen in the table, the amount of hydrocarbons increased in parallel with the increase in the irradiation dose (Table 2). Also, the increases of the hydrocarbons as a result of irradiation are given in Figure 1.

This finding concurs with those found by Hwang (1999) that 1-hexadecene, *1-7 hexadecadiene*, *n-pentadecane* and *1-tetradecene* were prominently detected in the irradiated sesame seeds after 0.5 kGy. Hwang (1999). Also, hydrocarbons *1-hexadecene*, *1-7 hexa-decadiene, n-penta-decane* were detected in pork, bacon and ham irradiated at 0.5 kGy or higher, but not in un-irradiated samples except for *1-hexadecene* (Park & Hwang, 1999).

Furthermore, hydrocarbon 1-tetradecene was not detected in un-irradiated peanuts, but was detected in nuts irradiated at 0.5 kGy or higher (Mexis & Kontominas, 2009a).

The authors found that the amount of stearic and palmitic acids increased while there was a decrease in the amount of oleic acid in parallel with the irradiation dose in walnuts (Mexis & Kontominas, 2009b). Irradiation doses applied to peanuts, pistachio nuts and hazelnuts resulted in an decrease in unsaturated fatty acids and parallel increase in saturated fatty acids. (Cam & Kilic, 2009; Mexis & Kontominas, 2009b).

Table 1. *Hydrocarbon contents of the irradiated hazelnut oils determined by gas chromatography*

Hydrocarbons	0kGy	0.5kGy	1kGy	3kGy	5kGy
1-tetradecene (ppm)	0.00	0.11	0.14	0.35	0.89
n-pentadecane (ppm)	0.00	0.12	0.26	0.51	1.02
1-7 hekzadecadiene (ppm)	0.00	1.61	2.76	5.32	10.42
1-hekzadecene (ppm)	0.00	0.16	0.52	0.71	2.01
n-eikosan (Internal standard)	4.00	4.00	4.00	4.00	4.00

Table 2*. The relation between irradiation and hydrocarbon content for hazelnut oils*

Hydrocarbon	**Linear equation**	$\mathbf{R^2}$
1-tetradecene	$y = 0.065\,x + 0.05$	0.990
n-pentadecane	$y = 0.193\,x + 0.015$	0.982
1-7 hexadecadiene	$y = 0.95\,x + 1.24$	0.947
1-hekzadecene	$y = 0.36\,x + 0.01$	0.918

y : amount of hydrocarbons(ppm)
x : irradiation dose (kGy)

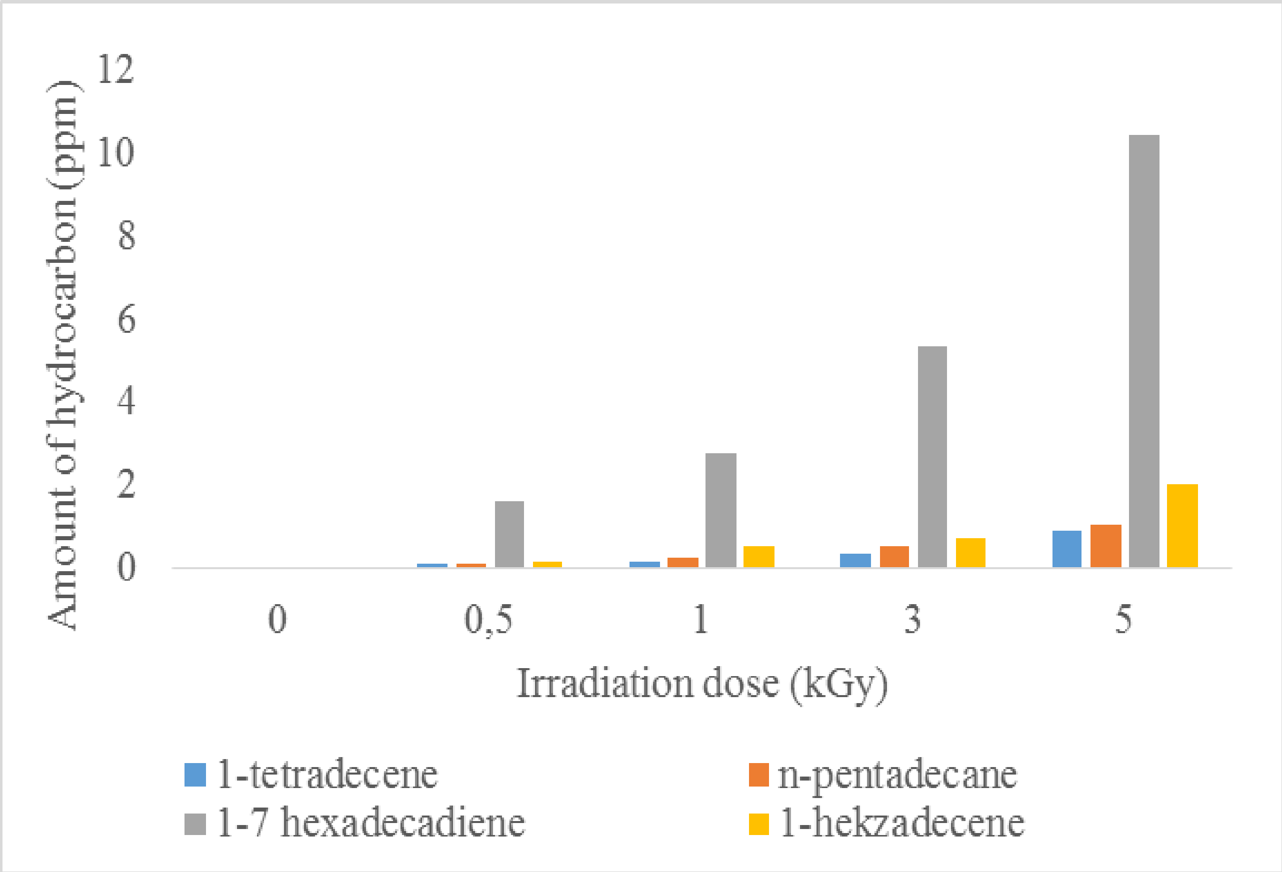

Figure 1. *Hydrocarbon contents of the irradiated hazelnut oils determined by gas chromatography*

The Rancimat prosess is generally used to measure the oxidative stability in oils. The stability of oils decreases as the amount of unsaturated fatty acids increases. The increase in the number of double bonds in the fatty acid makes it easier for free radicals to break the double bonds. Therefore, the excess of un-saturated fatty acids reduces the stability of oils.

The Rancimat prosess is generally used to measure the oxidative stability in oils. The stability of oils decreases as the amount of unsaturated fatty acids increases. The increase in the number of double bonds in the fatty acid makes it easier for free radicals to break the double bonds. Therefore, the excess of un-saturated fatty acids reduces the stability of oils.

The effects of gamma irradiation at various levels on the Rancimat values of hazelnut oils are shown in Table 3. The graph of the change in conductivity (mS/cm) against IT in hazelnut oils irradiated at different doses is given in Figure 2. As can be seen from the figure, when nut oils irradiated 5kGy, conductivity increase occurred in a shorter time compared to other irradiation doses.

In a study with oils, it was shown that, heat application, which causes oxidation in oils, increases the conductivity value (Yaşkıran, 2020). Also, while induction time detected in non-irradiated oils was 11.6 hours and induction time decreased 9.25 hours after 5 kGy irradiation (Figure 1). An induction time of 14.5 hours was reported in hazelnuts (Gecgel et al., 2011). The concentration of the total saturated fatty acids increased while the total amount of mono-unsaturated and poly-unsaturated fatty acids decreased with the different irradiation dose applied to black cumin seeds (Arici et al., 2007).

Table 3. *Determination of oxidative stability of irradiated hazelnut oils by the Rancimat Method*

Dose (kGy)	Induction time (h)
0.0	11.60
0.5	11.14
1.0	10.90
3.0	10.31
5.0	9.25
Regression equation	$y = 0.432\ x + 11.461$
Regression coefficient	$r^2 = 0.9785$

y : induction time(hour)
x : irradiation dose (kGy)

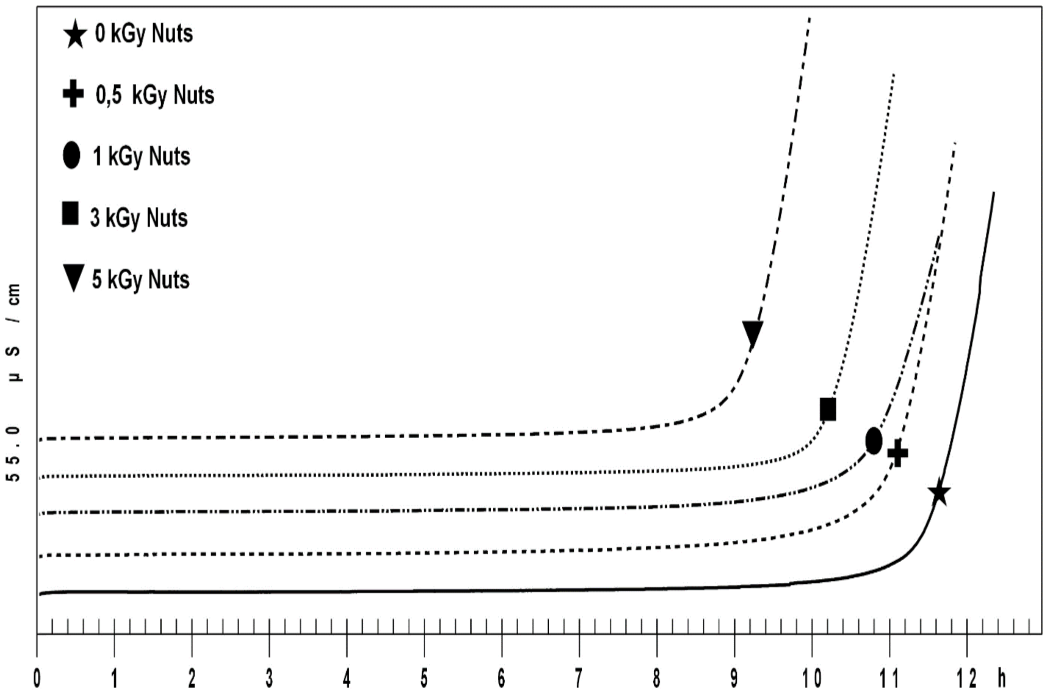

Figure 2. *Determination of oxidative stability of irradiated hazelnut oils by the Rancimat Method*

4. CONCLUSION

It was shown that the hydrocarbon content and oxidative stability of hazelnut oils depend on the irradiation dose applied. An adverse effect of gamma irradiation on induction times was observed. When irradiation dose increased, IT of the oil was decreased. Hydrocarbon formation was observed in the irradiated oils. The amount of hydrocarbon formed increased with increasing dose.

When oily foods are irradiated, the amount of hydrocarbons increases in parallel with the decrease in IT. There is a negative correlation between these two features.

Also, the results show that if the irradiation dose applied to hazelnut oils is known, IT, which is an important criteria for oils, can be determined by the formula given Table 1. In addition, If the irradiation dose applied to hazelnut oils is known, the amount of hydrocarbons in the oil can be determined by the formula given Table 2.

ACKNOWLEDGEMENT

Author would like to thank to the Turkish Energy, Nuclear and Mineral Research Agency.

CONFLICT OF INTEREST

No conflict of interest was declared by the author.

REFERENCES

Acheson, D., & Steele, J. H. (2001). Food Irradiation: A Public Health Challenge for the 21st Century. *Clinical Infectious Diseases*, *33*(3), 376-377. doi:10.1086/321899

Arici, M., Colak, F. A., & Gecgel, U. (2007). Effect of gamma irradiation on microbiological and oil properties of black cummin (*Nigella sativa* L.). *Grass Aceites.*, *58*(4), 339-343. doi:10.3989/gya.2007.v58.i4.444

Cam, S., & Kilic, M. (2009). Effect of Blanching on Storage Stability of Hazelnut Meal. *Journal of Food Quality*, *32*(3), 369-380. doi:10.1111/j.1745-4557.2009.00254.x

Chauhan, S. K., Kumar, R., Nadanasabapathy, S., & Bawa, A. S. (2009). Detection Methods for Irradiated Foods. *Comprehensive Reviews in Food Science and Food Safety*, *8*(1):4-16. doi:10.1111/j.1541-4337.2008.00063.x

Chmielewski, A. G. & Migdal, W. (2005). Radiation decontamination of herbs and spices. *Nukleonika*, *50*(4), 179-184.

Choi, C. R. & Hwang, K. T. (1997). Detection of Hydrocarbons in Irradiated and Roasted Sesame Seeds. *J. Am. Oil Chem. Soc.*,*74*(4), 469-472. doi:10.1007/s11746-997-0108-y

EN 1784:2003 (2003). Foodstuffs - Detection of irradiated food containing fat - Gas chromatographic analysis of hydrocarbons, withdrawn European Standard.

Farkas, J. (2004) Food Irradiation. In: A. Mozumder, Y. Hatano (Eds.), *Charged particle and photon interactions with matter* (pp. 785-812). Marcel Dekker Inc., New York-Basel.

Frank, J., Geil, J. V, & Freaso, R. (1982). Automatic Determination of Oxidation Stability of Oil and Fatty Products. *Food Technol.*, *36*, 71-76.

Gecgel, U., Gumus, T., Tasan, M., Daglioglu, O., & Arici M. (2011). Determination of Fatty Acid Composition of γ-irradiated Hazelnuts, Walnuts, Almonds, and Pistachios. *Radiat. Phys. Chem.*, *80*(4), 578-581. doi:10.1016/j.radphyschem.2010.12.004

Hasenhuettl, G. L., & Wan, P. J. (1992). Temperature Effects on the Determination of Oxidative Stability with the Metrohm Rancimat. *J. Am. Oil Chem. Soc.*, *69*(6), 525-527.

Hwang, K. T. (1999). Hydrocarbons detected in irradiated pork, bacon and ham. *Food Res. Int.*, *32*(6), 389-394. doi:10.1016/S0963-9969(99)00040-X

Kader, A. A. (1986). Potential application of ionizing radiation in postharvest handling of fresh fruits and vegetables. *Food Technology*, *40*(6), 117-121.

Loaharanu, P. (1994). Status and prospects of food irradiation. *Food Technology*, *52*, 124-131.

Mateos, R., Trujillo, M., Pérez-Camino, M. C., Moreda W., & Cert, A. (2005). Relationships between oxidative stability, triacylglycerol composition, and antioxidant content in olive oil matrices. *J. Agric. Food Chem.*, *53*(14), 5766-5771. doi:10.1021/jf0504263

Mendez, E., Sanhueza, J., Speisky, H., & Valenzuela, A. (1996). Validation of the Rancimat Test for the Assessment of the Relative Stability of Fish Oils. *J. Am. Oil Chem. Soc.*, *73*(8), 1033-1037. doi:10.1007/BF02523412

Mexis S. F., & Kontominas, M. G. (2009a.). Effect of γ-Irradiation on the Physicochemical and Sensory Properties of Walnuts (*Juglans regia* L.). *Eur. Food Res. Technol.*, *228*, 823-831. doi:10.1007/s00217-008-0995-7

Mexis, S. F., & Kontominas, M. G. (2009b). Effect of Gamma Irradiation on the Physico-chemical and Sensory Properties of Raw Shelled Peanuts (*Arachis hypogaea* L.) and Pistachio Nuts (*Pistacia vera* L.). *J. Sci. Food Agr.*, *89*(5), 867-875. doi:10.1002/jsfa.3526

Mexis, S. F., Badeka, A. V., Chouliara, E., Riganakos, K. A., & Kontominas, M. G. (2009). Effects of γ-Irradiation on the Physicochemical and Sensory Properties of Raw Unpeeled Almond Kernels (Prunus dulcis). *Innovative Food Sci. Emerg. Technol.*, *10*(1), 87-92. doi:10.1016/j.ifset.2008.09.001

Olson, D. G. (1998). Irradiation of food. *Food Technology*, *52*, 56-62.

Park, J. Y., & Hwang, K. T. (1999). Hydrocarbons as Markers for Identifying Postirradiated Peanuts. *J. Am. Oil Chem. Soc.*, *76*(1), 125-129. doi:10.1007/s11746-999-0058-7

Sádecká, J. (2007). Irradiation of Spices- a Review. *Czech J. Food Sci.*, *25*(5), 231-242.

Spiegelberg, A., Schulzki, N., Helle, N., Bögl, K. W., & Schreiber, G. A. (1994). Methods for Routine Control of Irradiated Food: Optimization of a Method for Detection of Radiation-Induced Hydrocarbons and Its Application to Various Foods. *Radiation Physics and Chemistry*, *43*(5), 433-444. doi:10.1016/0969-806X(94)90059-0

Thayer, D. W., Josephson, E. S., Brynjolfsson A., & Giddings G. G. (1996). Radiation Pasteurization of Food. *Council for Agricultural Science and Technology*, *7*, 1-10.

Tjaberg, T. B., Underdal, B., & Lunde, G. (1972). The effect of ionizing radiation on the microbial content and volatile constituents of spices. *Journal of Applied Bacteriology*, *35*(3), 473-478. doi:10.1111/j.1365-2672.1972.tb03724.x

URL1 (2019, October 03). Food Irradiation Legislation *"Gıda Işınlama Yönetmeliği"*. Official Gazette of the Republic of Turkey, No:30907. www.resmigazete.gov.tr/eskiler/2019/10/20191003-1.htm

URL2 (2012). Hazelnut Exportation from Turkey. Hazelnut Promotion Group. www.ftg.org.tr/en/turkish-hazelnut-hazelnut-export.html

URL3 (1999, Novermber 06). Food Irradiation Legislation *"Gıda Işınlama Yönetmeliği"*. Official Gazette of the Republic of Turkey, No:23868. www.resmigazete.gov.tr/arsiv/23868.pdf

WHO, World Health Organization (1994). Safety and nutritional adequacy of irradiated food. World Health Organization, Geneva. https://apps.who.int/iris/handle/10665/39463.

Yaşkıran, K. (2020). *Kızartmalık Mısırözü Yağı Kalitesinin İyileştirilmesinde Üç Farklı Turunçgil Albedosunun Suni Bir Antioksidan ve Adsorban ile Karşılaştırılması*. MSc Thesis, Necmettin Erbakan Üniversitesi Fen Bilimleri Enstitüsü.

Gazi University
Journal of Science
PART A: ENGINEERING AND INNOVATION
http://dergipark.org.tr/gujsa

Design and Finite Element Analysis of a New Kirschner Wire for Fixing Bone Fractures in Orthopedic Surgery

Canan İNAL[1], Kadir GÖK[2*], H. Deniz ADA[3]

[1]Kutahya Health Sciences University, Department of Anesthesiology and Intensive Care, Kutahya, Turkey
[2]Izmir Bakircay University, Engineering and Architecture Faculty, Department of Biomedical Engineering, Izmir, Turkey
[3]Dumlupinar University, Kutahya Vocational School of Technical Sciences, Chemical Technologies, Germiyan Campus, Kutahya, Turkey

Keywords

Salter Harris Type 3
A New Kirschner Wire Design
Finite Element Method
Fracture

Abstract

In this study, a new Kirschner wire (K-wire) design was performed to fix bone fractures in orthopedic surgery. The numerical analyses were completed based on the finite element method (FEM), using Deform-3D software. In this kind of numerical analyses using the FEM, friction, material model, the load and boundary conditions must be defined correctly. It has been seen that the new design is more advantageous in terms of implant failure or stability of fracture fixation. In addition, a good compatibility was found between the experimental results and the finite element analysis (FEA) results. This confirmed the accuracy of the finite element model. Therefore, this finite element model can be used reliably in drilling processes. We believe that with the use of new design investigated may have the role on the patients taking away from recurrent anesthesia and orthopaedic surgical risk.

Cite

İnal, C., Gök K., & Ada, H. D. (2022). Design and Finite Element Analysis of a New Kirschner Wire for Fixing Bone Fractures in Orthopedic Surgery. *GU J Sci, Part A, 9*(1), 41-48.

Author ID (ORCID Number)

C. İnal, 0000-0002-8119-6978
K. Gök, 0000-0001-5736-1884
H. D. Ada, 0000-0001-9991-8396

Article Process

Submission Date	01.02.2022
Revision Date	18.03.2022
Accepted Date	28.03.2022
Published Date	29.03.2022

1. INTRODUCTION

In our daily life, some injuries and bone fractures can occur in our musculoskeletal system due to any accidental trauma. These bone fractures can be treated by surgeons with conventional or surgical procedures depending on the condition of the fracture. If the treatment process of the fracture requires a surgical procedure after the bone fractures are reduced, they are fixed with plates using screws. First, bone drilling operations are performed with surgical drill bits suitable for screw sizes. During bone drilling, a heat is released due to the friction caused by the contact between the bone and the surgical drill bit. This heat causes undesirable conditions by increasing the temperature levels of the bone and surrounding soft tissues. This heat damage is known as necrosis. With necrosis, the bone remains bloodless. This situation reduces the success of implantation. The threshold value of this temperature level, which causes thermal damage, varies between 47°C and 55°C in the literature (Eriksson et al., 1984; Hillery & Shuaib, 1999; Augustin et al., 2008). The use of fluid to remove heat from the drilling site is undesirable due to the risk of infection (Hillery & Shuaib, 1999; Sezek et al., 2012).

There are existing studies in the literature. Most of these studies used surgical drill bits or K-wires and were related to temperature or necrosis caused by bone models. Some studies are concerned with optimum drilling parameters. According to Gok et al. (2015a) developed a new driller system to prevent osteonecrosis and performed optimization of drilling processing parameters of bone models (Gok et al., 2014a). Some studies have analyzed bone drilling with K-wire or surgical drill bits with FEA and compared them with experimental studies (Yuan-Kun et al., 2008; 2009; 2011; Alam et al., 2009). We can also see other studies in the literature.

*Corresponding Author, e-mail: kadir.gok@bakircay.edu.tr

These are fatigue behaviors of schanz screws, optimization processes, biomechanical effects of different configurations of K-wires (Gok et al., 2014b; Gok, 2015, Inal et al., 2019). In this study, a new K-wire design was performed to fix bone fractures in orthopedic surgery. A new K-wire design has been applied to Salter Harris (SH) type 3 epiphyseal fracture of distal femur and performed the FEA analyses (Figure 1).

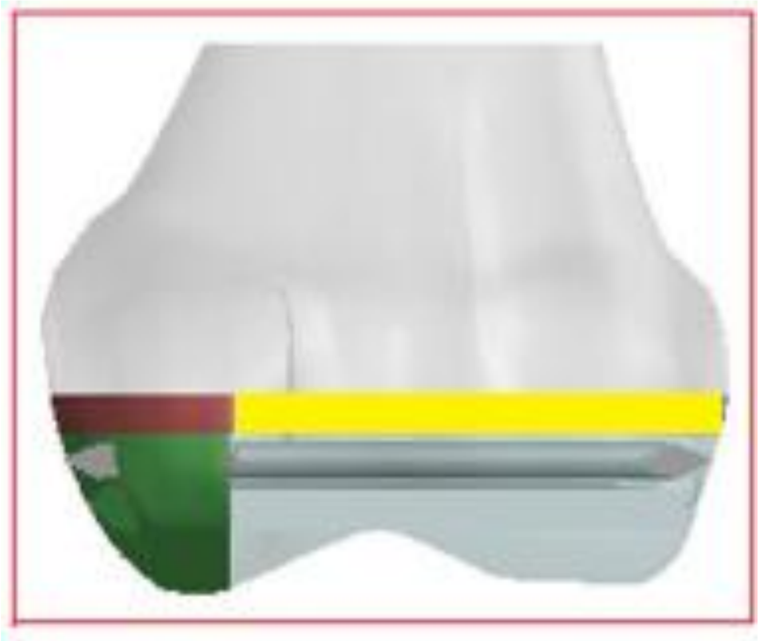

Figure 1. *K-wire with fracture model*

2. COMPUTER AIDED DESIGN AND FINITE ELEMENT ANALYSIS

In this study, three dimensional (3D) models of K-wires were created by SolidWorks and FEA analyses were performed in DEFORM-3D. The 3D models of K-wires were illustrated in Figure 2.

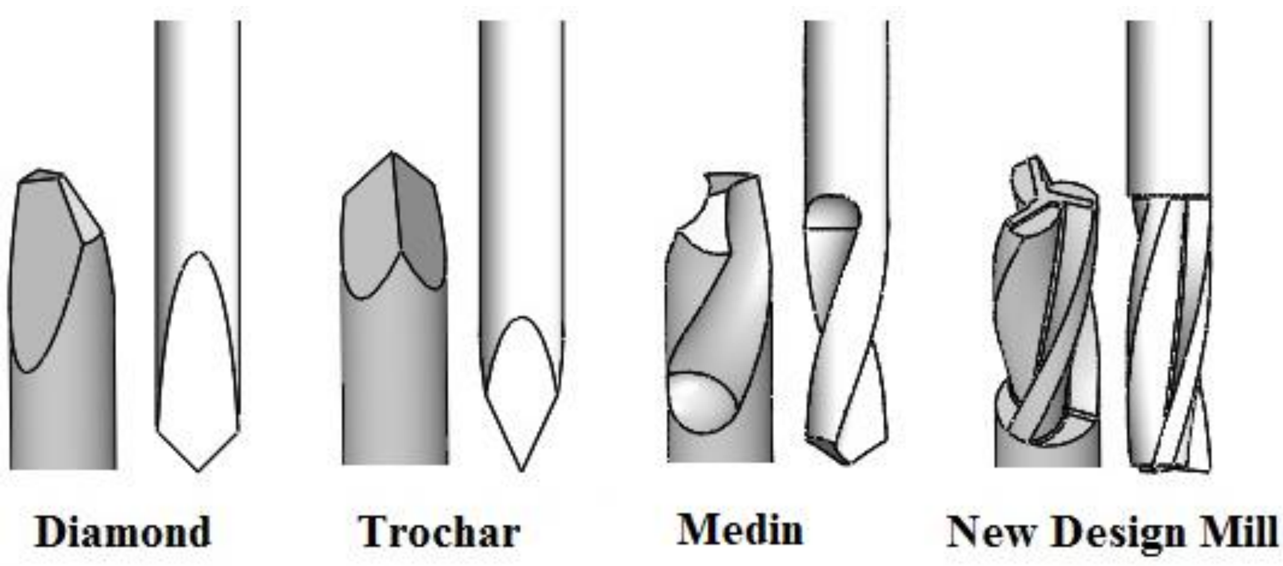

Figure 2. *The 3D models for K-wires*

2.1. Loading and Boundary Conditions

In mesh process (tetrahedral element), bone model has 21498 elements and 4853 nodes, K-wire has of 22958 elements and 5742 nodes. Boundary Conditions are illustrated in Figure 3a. The frictional contact type were defined and friction coefficient is 0.53 (Gok et al., 2015b). The bone model model was fixed from its outer surfaces. While the spindle speed was defined as 400 rpm and feed rate was set as 120 mm/min bit as seen in Figure 3b.

2.2. Material Model

While bone material properties were defined from , the stainless steel (AISI 304) was defined as K-wire from Deform-3D software (Deform_Material_Library, MatWeb, 2022). The flow stress curves McElhaney & Byars (1965) of bone models material model were given in Figure 4. The flow stress $(\bar{\sigma})$ was given in Equation (1). The effective plastic strain is $\bar{\varepsilon}$, the effective strain rate is $\dot{\bar{\varepsilon}}$, and temperature is T.

Drill bit used in orthopaedic procedures are not required to be as corrosion-resistant as implant materials, since they are not in contact with body fluids or tissues for long periods of time. It is much more important that they retain their cutting edge and withstand repeated sterilization scycles in an autoclave at temperatures of up to 135 °C (Hillery & Shuaib, 1999). However, since the K-wires stay in the fracture area throughout the fracture healing process, they must be resistant to reaction (corrosion) as a result of body fluids. Therefore, corrosion resistant and biocompatible stainless steel types are preferred.

$$\bar{\sigma} = (\bar{\varepsilon}, \dot{\bar{\varepsilon}}, T) \tag{1}$$

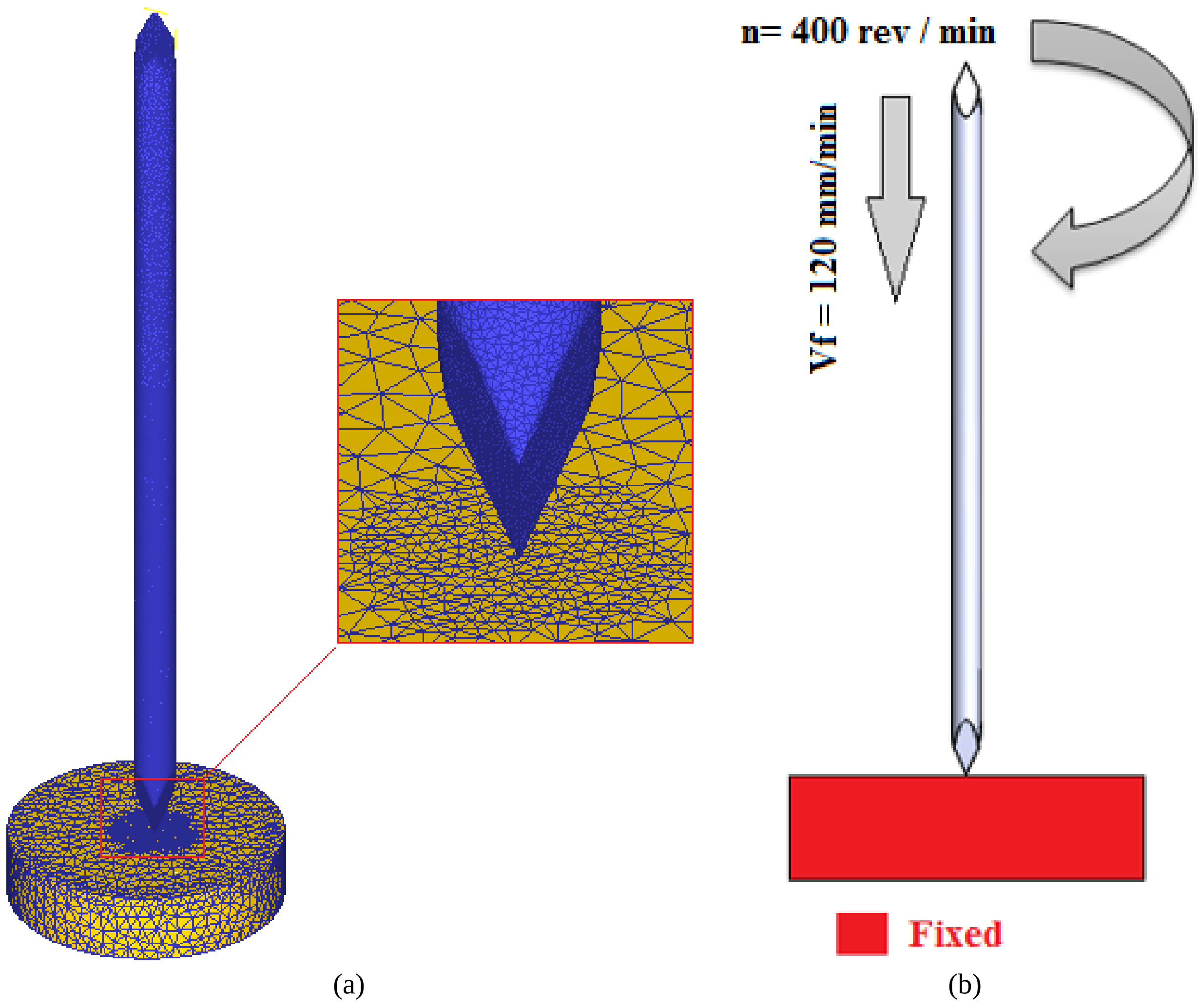

Figure 3. *Finite element model, **a)** mesh, **b)** the boundary conditions*

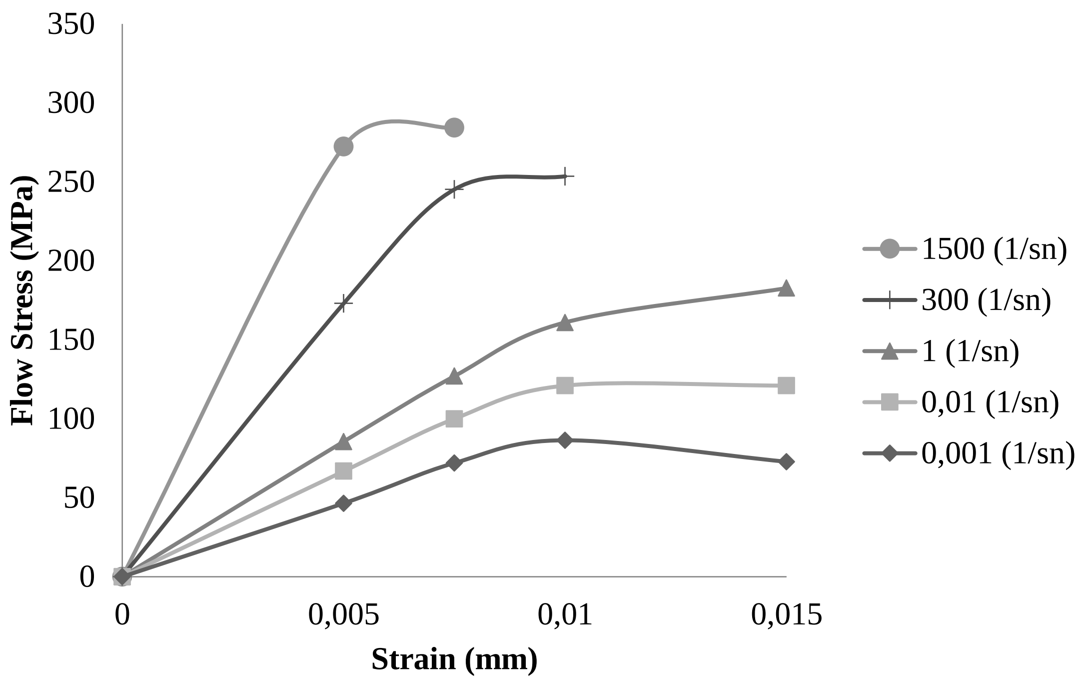

Figure 4. *Flow stress curves of bone models McElhaney & Byars (1965)*

3. RESULTS AND DISCUSSION

In orthopedic bone drilling, bone temperature levels are very important in terms of bone necrosis. The threshold value of this temperature has been determined as 47°C in the literature, otherwise, if the bone temperature level exceeds this value, permanent damage may occur in the bone and surrounding tissues. As illustrated in Figure 5, we have shown that the temperature graph obtained from drilling operations using K-wire designed such as milling cutter (new design) is lower than the others. The multi-edged of the K-wire increases the performance of the drilling process. Thus, it prevents the reaching of the critical temperature value (47ºC) which causes necrosis in the bone (Eriksson et al., 1984; Hillery & Shuaib, 1999; Augustin et al., 2008). Necrosis is a result of friction between the bone and the K-wire. This situation is not desired by surgeons too much. There are several methods to prevent this temperature. One of them is to choose the optimum cutting parameters. The other is to cool the drill bit, cutting tool or K-wire internally or externally. This work concentrated on developing the new K-wire design and performed drilling simulations on bone model samples using the K-wire.

Although the biomechanical behavior of different materials used in the implants could affect the stability, the design of drill bits or K-wires is also the other determinant factor in terms of thermal necrosis. The failure of implants can lead the patients to recurrent operations, and this also increases the anesthesia induced mortality and morbidity especially in older patients (Cottrell, 2008; Pignaton et al., 2016; Blaise Pascal et al. 2021; Çömez & Demirkıran, 2021). Globally, there were 178 million new fractures in 2019, with 455 million cases of common acute or long-term fracture symptoms reported. 25.8 million of them is mentioned as "years lived with disability of fractures" Wu et al. (2021). For this reason, successful fracture management becomes more important issue as many factors are related like fixation material designs for the stability.

Tool wear and damage mechanisms are critical to machining costs. Slower wear of tool tips extends tool life and reduces service costs. In addition, it is of high importance in terms of size and dimension tolerance of the processed material. In this respect, tool life is the most common criterion in terms of cutting tool performance and material machinability Stephenson & Agapiou (2018).

As result of drilling simulations, bone model temperatures were calculated as 61.1 (diamond type), 83.01 (trochar type), 53.90 (new design), 62.03 (medin), respectively. It was also illustrated in Figure 6, tool wear values were calculated for each K-wires. The crater wear occurred in k-wire was illustrated in Figure 7.

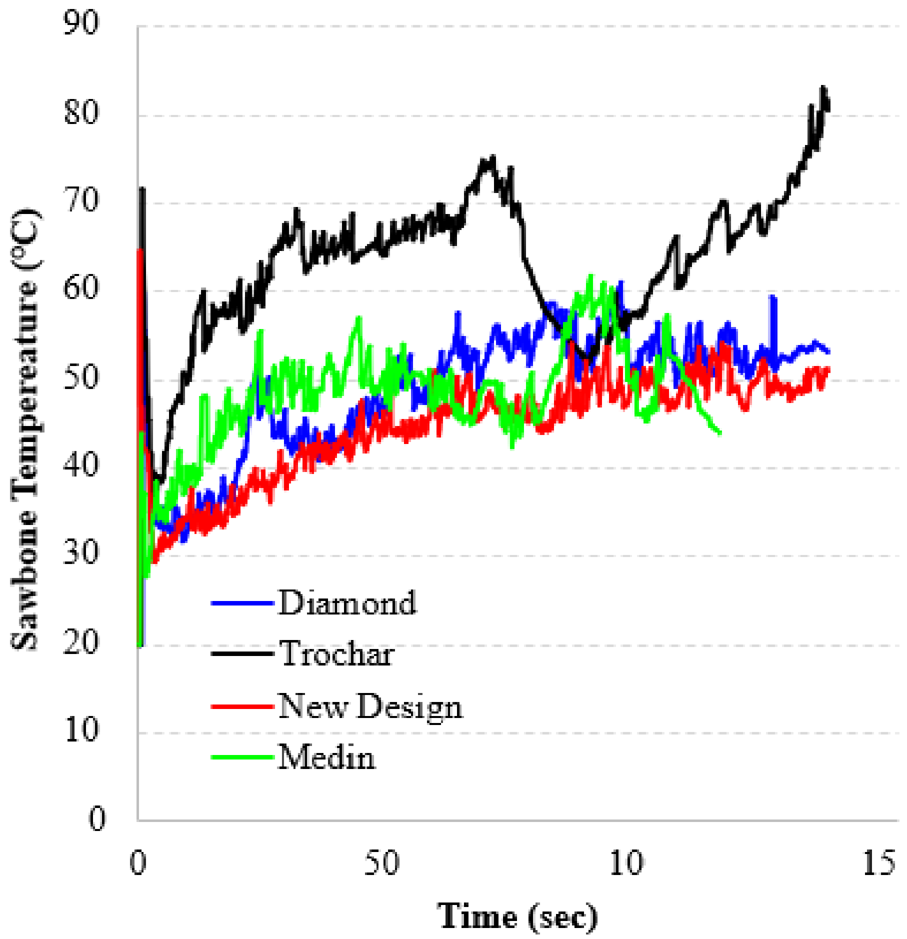

(a)

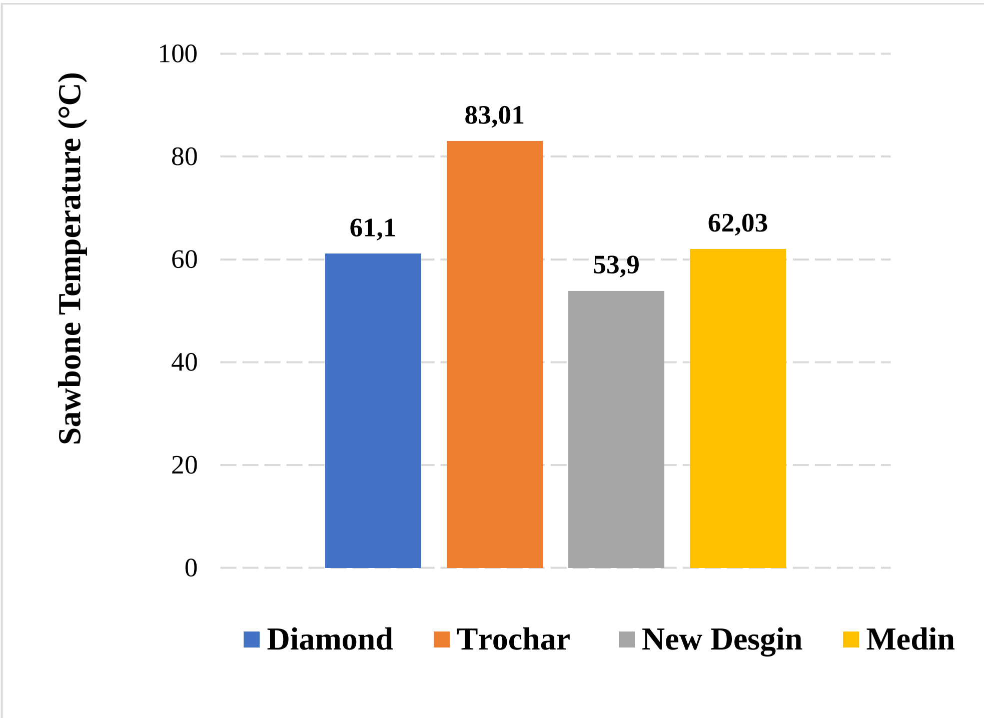

(b)

Figure 5. *Temperature changes in bone model as a result of drilling with different K wire models,* ***a)*** *variation to time,* ***b)*** *the highest temperature*

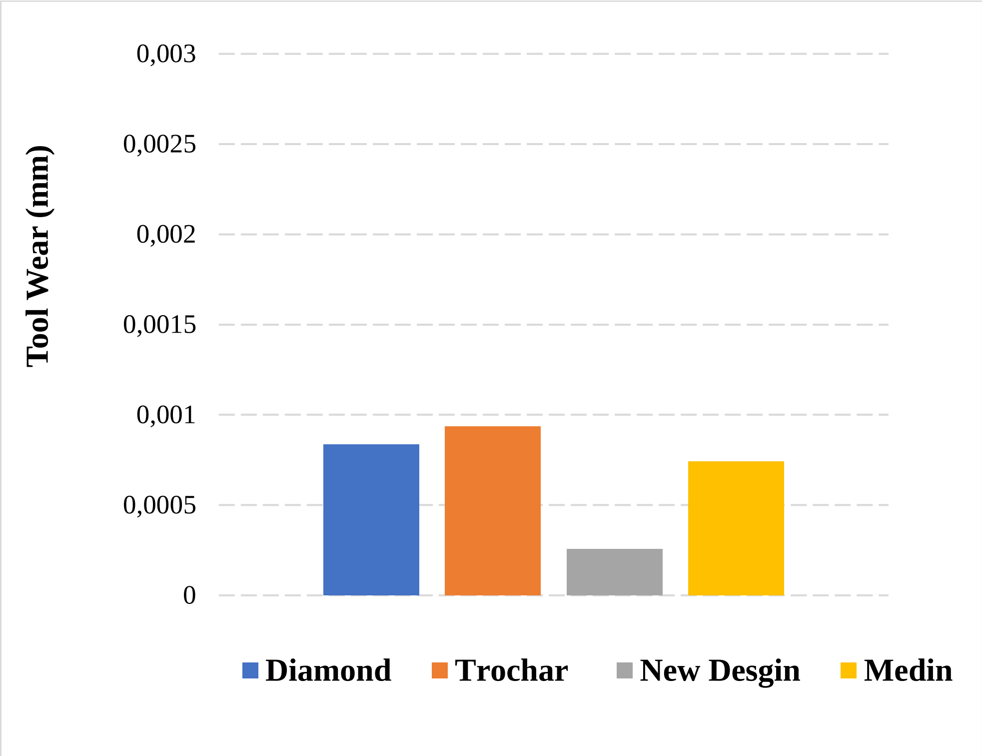

Figure 6. *The wear values occurred in K-wire*

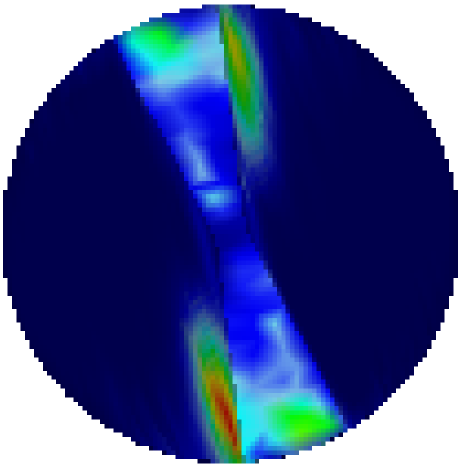

Figure 7. *The crater wear occurred in K-wire*

4.CONCLUSIONS

A new K-wire design used for stabilization after reduction of SH type 3 epiphyseal fractures of distal femur was developed and performed the FEA analyses. The results of the study indicate a significant solve for calculate to bone temperatures in drilling processes with K-wire. This model is likely to help in limiting the experiments required to determine of the bone temperatures during the drilling with K-wire. We believe that design of such implants must be investigated with more details in terms of thermal necrosis for fracture stability or others to prevent the patients from recurrent risk of anesthesia and orthopedic.

CONFLICT OF INTEREST

There is no conflict of interest

REFERENCES

Alam, K., Mitrofanov, A. V., & Silberschmidt, V. V. (2009). Finite element analysis of forces of plane cutting of cortical bone. *Comput. Mater. Sci.*, *46*(3), 738-743. doi:10.1016/j.commatsci.2009.04.035

Augustin, G., Davila, S., Mihoci, K., Udiljak, T., Vedrina, D. S., & Antabak, A. (2008). Thermal osteonecrosis and bone drilling parameters revisited. *Arch Orthop Trauma Surg*, *128*(1), 71-77. doi:10.1007/s00402-007-0427-3

Blaise Pascal, F. N., Malisawa, A., Barratt-Due, A., Namboya, F., & Pollach, G. (2021). General anaesthesia related mortality in a limited resource settings region: a retrospective study in two teaching hospitals of Butembo. *BMC Anesthesiology*, *21*(1), 60. doi:10.1186/s12871-021-01280-2

Cottrell, J. E. (2008). We Care, Therefore We Are: Anesthesia-related Morbidity and Mortality: The 46th Rovenstine Lecture. *Anesthesiology*, *109*(3), 377-388. doi:10.1097/ALN.0b013e31818344da

Çömez, M. S., & Demirkıran, H. (2021). Intraoperative Anesthesia-Related Mortality: A 10-Year Survey in a Tertiary Teaching Hospital. *Van Med J*, *28*(2), 280-287. doi:10.5505/vtd.2021.02259

Eriksson, A. R., Albrektsson, T., & Albrektsson, B. (1984). Heat caused by drilling cortical bone. Temperature measured in vivo in patients and animals. *Acta. Orthop. Scand.*, *55*(6), 629-631. doi:10.3109/17453678408992410

Gok, K., Gok, A., & Kisioglu, Y. (2014a). Optimization of processing parameters of a developed new driller system for orthopedic surgery applications using Taguchi method. *Int J Adv Manuf Technol.*, 76, 1437-1448. doi:10.1007/s00170-014-6327-0

Gok, A., Inal, S., Taspinar, F., Gulbandilar, E., & Gok, K. (2014b). Fatigue behaviors of different materials for schanz screws in femoral fracture model using finite element analysis. *Optoelectronics and Advanced Materials-Rapid Communications*, *8*(5-6), 576-580.

Gok, A. (2015). A new approach to minimization of the surface roughness and cutting force via fuzzy TOPSIS, multi-objective grey design and RSA. *Measurement*, *70*, 100-109. doi:10.1016/j.measurement.2015.03.037

Gok, K., Buluc, L., Muezzinoglu, U. S., & Kisioglu, Y. (2015a). Development of a new driller system to prevent the osteonecrosis in orthopedic surgery applications. *J Braz. Soc. Mech. Sci. Eng.*, *37*, 549-558. doi:10.1007/s40430-014-0186-3

Gok, A., Gok, K., & Bilgin, M. B. (2015b). Three-dimensional finite element model of the drilling process used for fixation of Salter–Harris type-3 fractures by using a K-wire. *Mech. Sci.*, *6*(2), 147-154. doi:10.5194/ms-6-147-2015

Hillery, M. T., & Shuaib, I. (1999). Temperature effects in the drilling of human and bovine bone. *Journal of Materials Processing Technology*, *92-93*, 302-308. doi:10.1016/S0924-0136(99)00155-7

Inal, S., Gok, K., Gok, A., Pinar, A.M., & Inal, C. (2019). Comparison of Biomechanical Effects of Different Configurations of Kirschner Wires on the Epiphyseal Plate and Stability in a Salter-Harris Type 2 Distal Femoral Fracture Model. *J Am Podiatr Med Assoc*, *109*(1), 13-21. doi:10.7547/16-112

MatWeb (2022). Searchable Database of Material Properties, http://www.matweb.com/

McElhaney, J., & Byars, E. F. (1965). *Dynamic response of biological materials*. American Society of Mechanical Engineers, New York.

Pignaton, W., Braz, J. R. C., Kusano, P. S., Módolo, M. P., de Carvalho, L. R., Braz, M. G., & Braz, L. G. (2016). Perioperative and Anesthesia-Related Mortality: An 8-Year Observational Survey From a Tertiary Teaching Hospital. *Medicine*, *95*(2), e2208. doi:10.1097/md.0000000000002208

Sezek, S., Aksakal, B., & Karaca, F. (2012). Influence of drill parameters on bone temperature and necrosis: A FEM modelling and in vitro experiments. *Comput. Mater. Sci.*, *60*, 13-18. doi:10.1016/j.commatsci.2012.03.012

Stephenson, D. A., & Agapiou, J. S. (2018). *Metal Cutting Theory and Practice*. CRC Press.

Wu, A.-M., Bisignano, C., James, S. L., Abady, G. G., Abedi, A., Abu-Gharbieh, E., Alhassan, R. K., Alipour, V., Arabloo, J., Asaad, M., Asmare, W. N., Awedew, A. F., Banach, M., Banerjee, S. K., Bijani, A., Birhanu, T. T. M., Bolla, S. R., Cámera, L. A., Chang, J.-C., … Vos, T. (2021). Global, regional, and national burden of bone fractures in 204 countries and territories, 1990-2019: a systematic analysis from the Global Burden of Disease Study 2019. *The Lancet Healthy Longevity*, *2*(9), e580-e592. doi:10.1016/s2666-7568(21)00172-0

Yuan-Kun, T., Li-Wen, C., Ching-Chieh, H., Yung-Chuan, C., Hsun-Heng, T., & Li-Chiang, L. (2008, May 16-18). *Finite element simulation of drill bit and bone thermal contact during drilling*. In: Proceedings of the 2nd International Conference on Bioinformatics and Biomedical Engineering (iCBBE 2008), Shanghai, China, (pp. 1268-1271). doi:10.1109/ICBBE.2008.645

Yuan-Kun, T., You-Yao, H., & Yung-Chuan, C. (2009). Finite element modeling of kirschner pin and bone thermalcontact during drilling. *Life Sci. J.*, *6*(4), 23-27.

Yuan-Kun, T., Wei-Hua, L., Li-Wen, C., Ji-Sih, C., & Yung-Chuan, C. (2011, May 10-12). *The effects of drilling parameters on bone temperatures: a finite element simulation*. In: Proceedings of the 5th International Conference on Bioinformatics and Biomedical Engineering (iCBBE 2011), Wuhan, China, (pp. 1-4). doi:10.1109/icbbe.2011.5780448

JOURNAL OF SCIENCE

PART A: ENGINEERING AND INNOVATION

GAZİ UNIVERSITY

1926

Correspondence Address

Gazi University
Graduate School of Natural and Applied Sciences
Emniyet Neighborhood, Bandırma Avenue
No:6/20B, 06560, Yenimahalle - ANKARA
B Block, Auxiliary Building

Yazışma Adresi

Gazi Üniversitesi
Fen Bilimleri Enstitüsü
Emniyet Mahallesi, Bandırma Caddesi
No:6/20B, 06560, Yenimahalle - ANKARA
B Blok, Ek Bina

e-mail | e-posta
gujsa06@gmail.com

web page | web sayfası
https://dergipark.org.tr/tr/pub/gujsa

e-ISSN 2147-9542